Submarine landslides – architecture, controlling factors and environments. A summary.

Nicola Scarselli

Fault Dynamics Research Group. Department of Earth Sciences, Royal Holloway University of London, Egham, TW20 0EX, Surrey, United Kingdom

ABSTRACT

Submarine landslides is a broad term for indicating the phenomena of failure of near seabed marine sediments under the effect of gravity. This occurs for the concomitance of external stresses applied to the sediments (triggering factors) and environmental conditions that weaken sediments (preconditioning factors).

Submarine landslides are typically classified on the basis of the type of failure movement that produced them. Recent classification schemes, however, divide those on the basis of the morphology of the resultant deposits (i.e. confined vs. frontally emergent failures) and on of the basis of the submarine physiographic region from which they initiate (i.e. attached vs. detached failures).

Despite the morphology of the deposits closely varies with the dominant collapse process, submarine landslides show a typical tripartite morphology with an updip headwall domain, a translational domain and a downslope toe domain. Each of these domains are typified by distinct structures which their interpretation could provide kinematic indicators for their evolution.

Several specific factors contribute to slope failure according to the environments where landslides occur. These factors can be categorized as triggering factors, if they act over a short period of time ultimately causing slope failure (e.g. earthquakes), or preconditioning factors if they arise during deposition and solely favour failure (e.g. stiff vs weak lithologies). Statistical studies of slope failure clearly show that most landslides occur on deep gentle slopes, with the largest ones found in seismically quiet areas. This implies that steepness of the slope and seismic activity are not the main factors that control size and distribution of landslides, but instead the combination of multiple preconditioning factors seems to be critical for failure initiation.

1 Introduction

Gravity-driven processes at continental margin occur at different scales producing a wide spectrum of products and styles (Butler and Turner, 2010). These vary from margin-scale megaslides can involve thicknesses of stratigraphy of several kilometres (see Rowan in this volume), to shallow submarine landslides that produce mostly incoherent deposits. The latter are the focus of this contribution.

When a pile of near-seabed marine sediment is subjected to external stresses or looses its internal strength, it fails under the effect of gravity producing a range of deposits that are collectively referred with various terms such as submarine landslides, mass transport complexes, mass transport deposits or slump complexes (Frey-Martínez et al., 2005; Gee et al., 2006; Hampton et al., 1996; Moscardelli et al., 2006; Posamentier and Martinsen, 2011). Submarine landslides remobilise and displace meters to hundreds of meters of sediments producing deposits that exhibit a basal shear surface above which material is translated down dip from a proximal headwall domain to a distal toe domain (Fig. 1 & 2).

The study of submarine landslides has been carried out using primarily outcrop and geophysical studies. Outcrop studies have offered significant insights into the emplacement processes, lithologic and kinematic details at the micro and meso scale (Alsop et al., 2017; Alsop and Marco, 2014; Alves and Lourenco, 2010; Bradley and Hanson, 1998; Butler and McCaffrey, 2010; Callot et al., 2008; Farrell and Eaton, 1987; García-Tortosa et al., 2011; Lucente and Pini, 2008, 2003; Martinsen, 1989; Martinsen and Bakken, 1990; Ogata et al., 2012; Strachan, 2002; Strachan and Alsop, 2006; Webb and Cooper, 1988; Woodcock, 1979). Geophysical techniques, such as 2D seismic and multibeam bathymetry, have allowed an understanding of the overall geometry and architecture of submarine landslides and have provided important statistical data (Booth et al., 1993; Canals et al., 2004; Dingle, 1980; Masson et al., 2002; McAdoo et al., 2000; Moore et al., 1994; Piper et al., 1985; Prior et al., 1979,

1982, 1984; D. B. Prior et al., 1986; Prior and Coleman, 1984; Twichell et al., 2009).

In the last 15 years, high-resolution 3D seismic surveys have been acquired along vast stretches of many unstable continental margins for exploration purposes. This has allowed the use of 3D seismic data to provide deep understanding of the internal variability of structures of submarine landslides at the macro scale (Bull et al., 2009; Frey-Martínez et al., 2006; Frey-Martínez, 2010; Frey-Martínez et al., 2005; Gafeira et al., 2010; Gee et al., 2006, 2007; Ireland et al., 2011; Jackson, 2011; Moscardelli et al., 2006; Moscardelli and Wood, 2008; O'Brien et al., 2018; Ortiz-Karpf et al., 2018a, 2018b; Richardson et al., 2011; Sawyer et al., 2009; Nicola Scarselli et al., 2013; Scarselli et al., 2016).

With a comprehensive set of geophysical examples of submarine landslides, this chapter is aimed at geoscientists that use the seismic methods to investigate sedimentary basins and wish to gain knowledge on the classification and architecture of submarine landslides and on the factors that control their emplacement.

2   Classifications

The classical classification scheme for submarine landslides is the one based on types of movement that can evolve from slope failure (e.g. Varnes 1958; Stow 1985; Nemec 1990). Recent studies have proposed that landslides can also be specifically classified on the basis of other criteria, such as their form of frontal emplacement (confined VS frontally emergent) (Frey-Martínez et al., 2006) and their sourcing regions (attached VS detached) (Moscardelli and Wood, 2008). This variety of classification schemes is here summarised.

Types of Movement
Many varieties of the classification of submarine landslides based on type of movement has been proposed in the literature in the last decades (Embley and Jacobi, 1977; Lee et al., 2007; Locat and Lee, 2002; McHugh et al., 2002; Mulder and Cochonat, 1996; Norem et al., 1990; Posamentier and Martinsen, 2011; Prior and Coleman, 1984; Stow, 1985; Varnes, 1958). This classification

identifies a set of end members of slope failure; these are creep, slide and slump (Fig. 3).

Creep is a slow strain failure due to constant load-induced stress (Stow, 1985). Creep can accelerate and eventually evolve into different types of failures such as slides and slumps (Fig. 3) (e.g. Stow 1986; Mulder and Cochonat 1996).

A slide does not involve important internal deformation of the failing mass during collapse. In contrast, a slump undergoes internal deformation during failure producing an internally contorted deposit (Fig.3). Sustained down slope movement of a slide can lead to brittle disintegration of the failing mass into smaller blocks hence generating a debris slide (Fig. 3) (McHugh et al., 2002).

Continued down slope movement of a debris slide or slump can result in mass disaggregation and sediment-water mixing that can transform the original failing mass in a debris flow (Fig. 3) (McHugh et al., 2002; Talling et al., 2007). Debris flows are surges of water and poorly sorted sediments present in equal volumes (e.g. Iverson 1997).

As fluid content increases due to continued downslope movement, a debris flow can evolve into a turbulent flow such as a turbidity current (Fig. 3) (e.g. Normark and Piper 1991; McHugh et al. 2002; Felix and Peakall 2006). In a turbidity current, sediment concentration is very low (0.1–7% by volume) and sediment particles are largely carried by fluid turbulence (e.g. Kneller and Buckee 2000; Meiburg and Kneller 2010). Turbidity currents can also be generated at a river mouth when the concentration of suspended sediment is large enough so that the density of the river water is greater than the density of sea water (e.g. Mulder and Syvitski 1995). For this reason, the inclusion of turbidity currents and their deposits as an end-member of submarine landslides has recently been questioned (Posamentier and Martinsen, 2011). Commonly, multiple failure events with similar or different type of movement can coexist within the same submarine landslide forming composite products (Mulder and Cochonat, 1996; Nicola Scarselli et al., 2013; Scarselli et al., 2020) (Fig. 4).

Frontally Confined VS Frontally Emergent Landslides

This classification is based on the morphology of the toe area of submarine landslides and has been proposed by Frey-Martínez et al. (2006) following extensive 3D seismic studies of submarine landslides on the continental margin of Israel (Eastern Mediterranean).

Frontally confined submarine landslides are totally entrenched within the surrounding undisturbed strata and exhibit a frontal thrust ramp with minimal displacement (Fig. 5a). For this reason, frontally confined submarine landslides are characterised by a low bathymetric relief and are thought to attain limited downslope transport of the failing mass. Downslope movement occurs by means of forward bulldozing of the foreland and formation of new frontal ramps basinward (Fig. 5a).

In contrast, frontally emergent landslides show prominent accumulation of the failing mass above the undisturbed strata at the toe region, caused by the ability of the basal shear surface to 'ramp up' stratigraphy and reach the seafloor (Fig. 5b). Frontally emergent landslides are hence characterised by high relief and significant downslope movement. The leading edge of these landslides can evolve into debris flows and turbidity currents.

Frontal emplacement and formation of a frontally emergent landslide seems to be controlled by the thickness of the landslide itself. This is because thin landslides have a shallow centre of gravity relative to seabed and therefore less energy is required for them to emerge. This seems to be supported by the fact that many of the frontally emergent landslides on the Israeli margin are relatively thin (≤100–150m). Also, steep slopes can provide enough driving force for landslides to emerge (Moernaut and De Batist, 2011).

Attached VS Detached Landslides

This classification was developed by Moscardelli and Wood (2008) following detailed 3D seismic analysis of Plio-Pleistocene submarine landslides from the continental margin of Trinidad and Tobago West Indies (Moscardelli et al., 2006; Moscardelli and Wood, 2008). The classification identifies two main categories of landslides, these are attached landslides and detached landslides (Fig. 6).

Attached landslides have their source areas located on (attached to) the margin of the basin that hosts them. This category is further divided into two subcategories, slope-attached landslides and shelf-attached landslides (Fig. 6a & b). Slope-attached landslides are derived from the catastrophic collapse of the upper slope that creates large headscarps in that portion of the margin (Fig. 6a). In contrast shelf-attached systems originates and are fed by large collapses of shelf edge deltas or by canyons that cut into the shelf edge (Fig. 6b).

Detached systems originate from any localized bathymetric highs within the hosting basin (Fig. 6c & d). For example detached landslides can occur from the flanks of mud volcanos, from oversteepened strata at the flanks of salt diapirs (Fig. 6c) or from oversteepened levees in channel-levee complexes (Fig. 6d).

Attached landslides are likely to be regional units covering thousand of square kilometres in area and reaching thicknesses in the order of hundreds of meters, whereas detached landslides are usually sub-regional units that occupy tens of square kilometres (Moscardelli and Wood, 2008). Scarselli et al. (2016) have documented the occurrence of large detached landslides offshore Namibia that have originated from structural highs tens of kilometres wide related to basin-scale megaslides. This indicates that contingent to the size of the associated relief, detached landslides can attain extremely large volumes, sometime in excess of several hundreds cubic meters.

3   Structural Architecture of Submarine Landslides

Submarine landslides usually exhibit a tripartite anatomy that consist of an updip headwall domain, a translational domain and a downslope toe domain (Fig. 1). Outcrop and geophysical studies have indicated that these domains are typified by a variety of structures, some of which can be used as kinematic indicators for the dynamic evolution of landslides (Bull et al., 2009). The key structures that define the architecture of landslides are presented in the following paragraphs and are grouped according to the domain in which are likely to occur (Fig. 7). For a full review of internal structures of submarine

landslides the reader should consult Bull et al. (2009) and references within, from which most of this section is derived.

Headwall Domain

Two are the main structures that characterise the headwall domain, these are "headwall scarps" and "extensional ridges and blocks" (Figs. 1 & 7a & b).

Headwall scarps are the boundaries between landslides and undeformed, upslope strata (Fig. 7a). Headwall scarps are extensional failure surfaces that vertically cut stratigraphy and link at depth to the basal shear surface (Fig.7a). In plan-view, they may exhibit scoop-shaped or complex sinuous geometries (Figs. 2a & 7a). As the collapsing material is evacuated away from the headwall scarps, the identification of these structures reveals the gross transport direction of the associated landslides; this is generally perpendicular to the strike of the headwall scarps (Fig. 7a).

Extensional features, such as blocks or elongated ridges separated by normal faults, are usually observed close to headwall scarps (Figs. 7b & 8). These features represent coherent portions of stratigraphy that have been evacuated from headscarps. Elongated ridges are usually parallel to the associated headscarps, therefore the transport direction is usually perpendicular to the long axis of the ridges (Figs. 7b & 8). Spacing, disaggregation and reorientation of blocks and ridges usually increases with increasing distance away from the associated headscarp, limiting the use of these structures as reliable kinematic indictors.

Translational Domain

The downslope translation of the collapsed material can lead to intense deformation promoting the formation of several structural features, these include lateral margins, ramps & flats of the basal shear surface, basal grooves, internal longitudinal shear zones, folds and translated blocks (Figs. 1 & 7c-h).

Lateral margins are the lateral boundaries that divide landslides from undeformed, adjacent strata (Fig. 7c). They usually appear as dip parallel, continuous features that link with the headwall and toe domain (Figs. 1 & 7c).

Lateral margins are slip surfaces with a major component of oblique slip that laterally link extension and contraction within landslides. Since lateral margins laterally constrain landslides, their identification gives a fairly precise indication of the transport direction; that is down dip and parallel to these features (Fig. 7c).

Ramps & flats and grooves are features that are associated with the morphology of the basal shear surface (Figs. 7d & e). Ramps are defined as steep segments of the basal shear surface that cut up or down through stratigraphy, flats instead are segments of the basal shear surface that are parallel to the bedding, interposed between ramps (Fig. 7d). Flats occur along two or more preferred stratigraphic levels indicating the presence in the stratigraphy of multiple low friction surfaces that can be exploited as a basal shear plane. Ramps & flat can develop either perpendicular or parallel to the transport direction (Fig. 7d). The latter form elongate features that are usually referred as 'slots'. Even if ramps & flats are recurrent features, especially in large landslides, the mechanism behind their formation is yet not fully understood. It has been suggested that local lateral variations in friction of potential shear planes can control the stratigraphic location of the basal shear surface and therefore the formation of ramps & flats.

Basal grooves or striations are linear to sinuous depressions of the basal basal shear surface (Fig. 7e). These features can extend laterally for several kilometres and are usually oriented downslope. It is believed that such structures form as result of basal scouring by means of tools or coherent blocks embedded in the failing mass of the landslide. The depth and the cross-sectional shape of the grooves is controlled by the shape and size of the tools that generated the scours. Grooves can reach up to tens of meters in depth and vary in shape from cuspate to rounded. Grooves are very useful kinematic indicators as their length provides a rough estimation of the landslide runout and a precise indication of the transport direction (Fig. 7e). Occurrence of multiple sets of striations at the base of slumps are indicative of shifts in their internal transport direction (Fig. 9). These may be related to late collapse of the flanks of the failure or, alternatively, inward collapse of the whole system during

the waning phase of failure. This highlights the potential of striations to help reconstruct the strain history of complex events.

Longitudinal shear zones are continuous lineaments that occur in pairs and extended along the length of a landslide (Fig. 7f). The nature of these lineaments can be complex. They can consist of subtle elongate ridges or depressions at the top surface of landslides. Alternatively they be manifest as subtle boundaries that laterally divide portions of the failing mass characterised by different internal facies (Fig. 7f). Longitudinal shear zone are thought to represent boundaries of distinct segments of failure within a landslides that collapse at different time or at different strain rate. Similarly to lateral margins, longitudinal shear surfaces provide information about the transport direction of the failing mass, which will be down dip and parallel to the these structures (Fig. 7f).

Folds in landslides have been extensively reported by numerous field based studies (e.g. Alsop et al., 2019, 2017; Bradley and Hanson, 1998; Strachan and Alsop, 2006). Fold style in landslides can show considerable variation from upright symmetric folds to asymmetric, isoclinal and sheath folds.This variety in structural style of slump folds has been related to the degree of translation of the failing masses. Upright folds typify landslides that experienced little translation, complex folds such as isoclinal, sheath and refolded folds are common in more translated and hence more deformed landslides.
The downslope movement of a failing mass initiates trends of folds that are perpendicular to the transport direction and therefore perpendicular to the paleoslope direction (Fig. 7g). For this reason, slump folds are excellent kinematic indicators especially if the folds shown some degree of asymmetry. In this case, the vergence of the folds will provide the sense of the transport direction (Fig. 7g).

Translated blocks are coherent portions of stratigraphy that have been transported within the failing mass of a landslide (Fig. 7h). Translated blocks can undergo increasing deformation with increasing translation. Deformation can occur by means of disruption of internal stratigraphy, block rotation and reorientation. Translated blocks that have travelled for sufficiently long

distances tend to be aligned with their long axis parallel to the transport direction providing useful information on the kinematics of the hosting landslide (Fig. 7h).

Toe Domain

Pressure ridges and fold and thrust systems are the main structures that may occur at the toe domain of landslides (Fig. 7i & l). Both features form as a result of the contractional stress that develops at the toe of landslides. The difference between the two reside in the scale at which they occur.

Pressure ridges are linear to arcuate ridges that form at the top surface of a landslide due to the emplacement of metre- to tens of metre-scale thrust fault systems (Fig. 7i). They are usually seen associated with frontally emergent landslides and their identification gives an indication of transport direction that usually is orthogonal to these features (Fig. 7i).

Fold and thrust systems up to hundreds of metre in scale are commonly seen at the toe domain of thick frontally emergent submarine landslides (Fig. 7l). As pressure ridges, fold and thrust systems are very good kinematic indicators. Transport direction can be inferred from the vergence of the thrusts and the associated folds (Fig. 7l).

4   Mechanics of Slope Failures, Pre-conditioning and Triggering factors

A submarine landslide initiates when the driving stresses applied to a sediment column exceeds its shearing resistance (e.g. Hampton et al. 1996; Locat and Lee 2002; Lee et al. 2007). Slope failure is therefore favoured by (1) an increase in the driving stresses, (2) a decrease in shearing resistance or (3) a combination of the two (Lee et al., 2007). There are several natural factors that can increase the driving stresses and reduce the shear strength of sediments and they will be reviewed in the following paragraphs and summarised in Table 1).

These factors can be either seen as triggering factors, if they act in a relatively short period, ultimately triggering failure, or pre-conditioning factors, if they are acquired during the depositional process, favouring slope instability (Tab. 1)

(Canals et al., 2004; Leynaud et al., 2009; Masson et al., 2010).

Slope Steepening

Gravity exerts a downslope driving stress (gravitational shear stress) as long as the seafloor is not flat (Hampton et al., 1996; Lee et al., 2007; Locat and Lee, 2002). A steep slope is considered a preconditioning factor, whereas the increase of slope steepness is a plausible triggering factor (Huhnerbach et al., 2004; Masson et al., 2010; van Weering et al., 1998).

Slope steepening can result from tectonic deformation, sediment accumulation and erosion (e.g. Lee et al. 2007). Faulting, folding and diapirism (Fig. 10) causes local steepening of the seafloor that can lead to slope instability (Gee et al., 2006; Katz et al., 2015; McAdoo et al., 2000; Morley, 2009; Moscardelli and Wood, 2008; Scarselli et al., 2016; Welbon et al., 2007). Gravitational shear stress can increase also because more sediment accumulates at the head of a sloping surface than at the toe (Lee et al., 2007). Erosion at the toe of a sloping surface, for example by means of along-slope currents, increases the overall steepness of the slope therefore favouring collapse (e.g. Sayago-Gil et al., 2010; Tournadour et al., 2015).

Pore Fluid Pressure

Pore fluid pressure reduces the shear strength of sediment (Eqns. 1 & 2). High sedimentation rate, biogenic decay of organic matter, dissociation of gas hydrate and fluid seepage can all lead to an increase in pore fluid pressure in shallow sediments. The shear strength of sediments is in fact function of the effective vertical stress σ', the coefficient of friction μ and cohesion c (Terzaghi, 1962):

$$\tau = \sigma' \mu + c \quad \text{(Eqn. 1)}$$

The effective vertical stress is the total stress applied to the rock σ minus the effect of the pore fluid pressure u_w (Terzaghi, 1962):

$$\sigma' = \sigma - u_w \quad \text{(Eqn. 2)}$$

Therefore, high pore fluid pressure reduces the effective stress (Eqn. 2), and

hence the shear strength reduces too (Eqn. 1). In case of development of extreme overpressure the pore fluid pressure can approach the lithostatic pressure (i.e. $u_w \approx \sigma_v$) making sediments extremely weak (Eqns. 1 & 2).

Mud volcanos, pipes and associated pockmarks are indirect evidences of widespread overpressures in sedimentary basins (Fig. 11) (Huuse et al., 2010; Morley et al., 2011; Rowan et al., 2004). Overpressured fluids tend to migrate vertically along faults; lateral and vertical pathways are also provided by permeable stratigraphic levels that in turn may feed shallow pipes. Upward migration of methane-bearing fluid from deeper sources can cause shallow accumulations of gas hydrates that in seismic sections are marked by bottom simulating reflectors (Fig. 11) (e.g. Davie and Buffett, 2003).

Carbon dioxide, hydrogen sulphide, ethane and methane are gases that can derive from organic rich sediments by bacterial processes (e.g. Floodgate and Judd 1992; Fleischer et al. 2001). Although the biogenic production of gas is relatively slow, over a long period of time the amount of gas produced can be significant and can lead to excess pore pressures (Floodgate and Judd, 1992; Osborne and Swarbrick, 1997).

Dissociation of gas hydrate can build up excess of pore fluid pressure within the hosting sediments (Mienert et al., 2005, 1998; Xu and Germanovich, 2006). Gas hydrates are found along the slope of many continental margins where low temperatures and high pressures at the seabed provide the right physical conditions for their accumulation (e.g. Kvenvolden 1993). Modelling studies have shown that while deep-water gas hydrate deposits are stable under rapid variation of pressure and temperature at the seafloor (water depth > 500 m), shallower deposits can undergo rapid dissociation leading to high overpressures within the sediments hosting the gas hydrate (Kvenvolden, 1993; Milkov et al., 2000; Reagan and Moridis, 2007; Xu and Germanovich, 2006).

Excess pore pressures can result from lateral and vertical seepage of overpressured fluids and gas. Along near shore areas lateral groundwater seepage from coastal aquifers can be a likely trigger for landslides (Hampton et al., 1996; Lee et al., 2007; Locat and Lee, 2002; Masson et al., 2010). In particular, low tides and heavy rainfalls are able to induce accelerated seepage

of groundwater to the coast and cause anomalous high pore pressures within coastal shallow water sediments (e.g. Kopf et al. 2010).

On passive margins, lateral advection of fluids and gas can be established from the base of thick, overpressured sediment piles on the upper slope towards the lower slope, favouring the collapse of deep-water landslides (Dugan and Flemings, 2002, 2000; Flemings et al., 2008; Masson et al., 2010).

Amongst all the mechanisms that can cause excess fluid pressures, dissociation of gas hydrate and fluid seepage (especially if linked to tides) are considered effective triggering mechanisms for slope failure (Canals et al., 2004; Horozal et al., 2017; Masson et al., 2010). However, despite the abundant literature linking fluid overpressure to sediment failure, recent studies indicate that focused fluid flow features, such as pockmarks and pipes, can effectively drain sediments, recovering their strength, hence inhibiting their potential to fail (Riboulot et al., 2019).

Earthquakes
Earthquake shaking generates accelerations of the sediment column inducing shear stresses that can add to gravitational shear stresses, triggering the collapse of a stable slope (Hampton et al., 1996; Lee et al., 2007; Locat and Lee, 2002). Earthquake related stresses can also cause excess pore pressure leading to a degradation of shear strength of the sediment column (Biscontin et al., 2004; Lee et al., 2007). Enhanced shear stress and degraded shear strength due to seismic shaking make earthquakes a very effective trigger of submarine landslides.

Despite that, it has been shown that repeated, non-failure, seismic events can enhance shear strength through the development of excess pore pressures and subsequent drainage during successive earthquakes, resulting in a densification of the sediment column (Boulanger, 2000; Boulanger et al., 1998). This process is usually referred in the literature as "seismic strengthening" (Locat and Lee, 2002; Sawyer and DeVore, 2015).

Waves

The propagation of a wave train produces a non-uniform pressure field between crest and trough that induces shear stresses at the seabed (Henkel, 1970; Jeng, 2003, 2001; Seed and Rahman, 1978). Large waves generated during storms and hurricane are able to cause shear failure in soft sediments in water depths up to about 100 m (Bea et al., 1983; Henkel, 1970). Large waves generated during tsunamis or storms are considered to be a very effective triggering factor for submarine landslides (Canals et al., 2004; Lee et al., 2007; Masson et al., 2010). Internal waves that form in stratified oceanic water masses can be responsible for deep water landslides (Gavey et al., 2017; Huhnerbach et al., 2004; Reeder et al., 2011).

Sediment types

Sediment types and strength of sediment is thought to be a crucial factor for the development of submarine landslides. For example, weak shaly sediments, especially if saturated or overpressured, are prone to collapse and form large failures (e.g. Huhnerbach et al., 2004; Rodríguez-Ochoa et al., 2015).

Deposition from steady currents confer good sorting to contourite deposits, which implies higher water content in the sediments and hence their weakness (Laberg and Camerlenghi, 2008). Therefore, the widespread occurrence of contourites may represent an important preconditioning factor for landslides that have affected slopes where substantial deposition has been from bottom currents.

Recent research also indicates that altered volcanic deposits might form weak units which are candidate for localising the formation of basal shear surface of submarine landslides (Miramontes et al., 2018). Geotechnical investigation has in fact revealed that zeolitic layers, commonly formed by the alteration of volcanic rocks, tent to be anomalously highly porous. This allows for these units reaching water content similar to that of surface sediments, making them extremely weak and subject to failure.

5   Environments

The extensive research that has been carried out on submarine landslides

worldwide indicates that slope failure commonly occurs in five environments or landslides territories: fjords, deltas, submarine canyons, continental slopes and oceanic volcanic islands (e.g. Hampton et al. 1996; McAdoo et al. 2000; Mienert et al. 2002; Lee et al. 2007). These environments are intrinsically controlled by specific geological factors, which may provide triggering and preconditioning mechanisms for the submarine landslides there found.

Fjords

Fjord are narrow and elongate inlets with cliffs, created in a valley carved by glacial activity. Fjords are commonly characterised by energetic tides and show a steep fjord-head delta that is fed by sediment-laden rivers and streams that drain the diminished glacier that eroded the valley (e.g. Farmer and Freeland 1983; Syvitski et al. 1987; Syvitski and Farrow 1989).

The likely factors that favour failure in fjords are mainly related with the generation of excess pore pressure, these include high sedimentation rates at the fjord-head delta, accelerated groundwater seepage during low tides and biogenic decay of organic matters contained in the deltaic sediments (Bornhold and Prior, 1989; Hampton et al., 1996; Lee et al., 2007; D. B Prior et al., 1986; Stoker et al., 2010). Earthquakes can also play a major role in initiating submarine and subaerial failures along the steep slopes of fjords (Fig. 12) (Lastras et al., 2013).

Deltas on Continental Margins

Rivers with high sediment load entering a low energy marine environments can create thick wedges of shallow submarine deltaic sediments (e.g. Wright et al. 1973; Coleman 1976; Prior et al. 1986; Alexander et al. 1991; Kuehl et al. 1997). These deposits are commonly affected by slope failures as result of a combination factors (Hampton et al., 1996; Lee et al., 2007). High sedimentation rate and decaying of organic matter can lead to excess of pore pressure and a state of extreme underconsolidation. These thick and weak piles of sediments are therefore easily subject to gravitational collapse when loaded by external forces such as earthquakes and storm waves.

Submarine Canyons

Submarine canyons are the primary conduits for the transport of large amounts of sediment into the deep sea (e.g. Shepard 1972; Shepard 1981; Normark and Carlson 2003). Most submarine canyons are V-shaped, deeply incised with tall and steep walls and extend from the shelf to the deep-water where they are linked to large submarine fans (e.g. Stow and Mayall 2000; Normark and Carlson 2003).

Landslides often occur on the steep sidewalls of canyons, with the headscarps sub-parallel to the canyon axis (Antobreh and Krastel, 2006; Cunningham et al., 2005; Lastras et al., 2009; McAdoo et al., 2000) (Fig. 13). Failure is ascribed to oversteepening due to canyon floor incision and possibly favoured by earthquakes and storm waves (e.g. Hampton et al. 1996; McAdoo et al. 2000; Lee et al. 2007).

It is thought that "slope-confined canyons" or "headless canyons", i.e. submarine canyons that are not linked with the shelf (Bertoni and Cartwright, 2005; Orange and Breen, 1992; Twichell and Roberts, 1982), can evolve from the seafloor scouring created by the collapse of submarine landslides (Bertoni and Cartwright, 2005; He et al., 2014; Lee et al., 2007; Locat and Lee, 2002; Orange et al., 1997). This highlight the importance of submarine landslides in shaping the architecture of offshore margins.

Open Continental Slopes

Continental slopes form a large portion of continental margins that lie at water depths ranging from ~ 100 m to ~ 3000 m with an average slope of ~ 4° (e.g. Nittrouer 2007). Landslides occur on almost every continental slope, from active to passive margins, from glaciated to non glaciated margins (Camerlenghi et al., 2010; Canals et al., 2004; Lee, 2009; Lee et al., 2007; Leynaud et al., 2009; McAdoo et al., 2000; Mienert et al., 2002; Twichell et al., 2009).

Submarine landslides that occur on the slopes of active margins are favoured by several factors, including excess pore pressure induced either by tectonic compression and dissociation of gas hydrates, slope steepening related to the

emplacement of large thrusts and seismic activity (Ellis et al., 2010; McAdoo et al., 2000; Orange et al., 1997). Studies of high quality bathymetric data in the frontal part of accretionary wedges suggest that subduction of seamounts produce uplift of the bulging of the sedimentary cover of the overriding plate, causing extensive landslides (Pedley et al., 2010; Ruh, 2016).

Slope failure on passive margins is driven by several factors that induce overpressure generation and slope steepening. On passive margins, excess pore pressure is linked mainly with high sedimentation rates, seepage and gas hydrate dissociation (Masson et al., 2010, 2006; Mienert et al., 2002), while slope steepening is created by sediment accumulation and diapirism (McAdoo et al., 2000; Twichell et al., 2009) (Fig. 10).

Although passive margins are characterised by limited seismic activity, glaciated passive margins can be intensely affected by seismic shaking due to post-glacial isostatic rebound (Canals et al., 2004; Lee, 2009; Leynaud et al., 2009). Along continental slopes wave loading is seldom a major triggering factor (Bea et al., 1983; Henkel, 1970; Lee et al., 2007); in ultra deep-water gas hydrate are stable, therefore in this environment these can be discharged as the main factor leading to overpressure generation and slope failure (e.g. Xu and Germanovich 2006).

Oceanic Volcanic Islands
Oceanic volcanic islands are the tops of gigantic volcanic mountains formed by eruptions over several million years of basaltic lava generated in the upper mantle; some tower more than 9 km above the sea floor and have steep flanks that extend underwater for thousands of meters (e.g. Tilling et al. 1987; Tilling and Dvorak 1993) (Fig. 14).

Slope failure is very common on the flanks of many volcanic oceanic islands (Chadwick et al., 2012; Counts et al., 2018; Hampton et al., 1996; Lee et al., 2007; Locat and Lee, 2002; Masson et al., 2006) and is a fundamental process that profoundly controls the geomorphology and evolution of these oceanic volcanic mountains (Karstens et al., 2019; Mitchell et al., 2002) (Fig. 14).

Although landslides on the flanks of oceanic volcanic islands have been

intensely studied because of their tsunamigenic potential the causes of flank failure are relatively poorly understood (Masson et al., 2006). Many factors may combine and produce a trigger for landslides during the development of oceanic volcanos; these include catastrophic eruptions, eruption-related seismicity, slope steepening due to accumulation of eruptive products and magma chamber inflation and pore pressure build up due to dyke injection (Hürlimann et al. 2000; Masson et al. 2002 and references therein).

6   Statistics of Submarine Landslides

A fairly large amount of statistical information has been produced for submarine landslides from different environments and geological settings (Booth et al., 1993; Camerlenghi et al., 2010; Chaytor et al., 2009; Huhnerbach et al., 2004; Masson et al., 2002; McAdoo et al., 2000; Twichell et al., 2009).

The largest landslides occur mainly on open continental slopes and on oceanic island flanks where failures can attain volumes in the order of 1000 km^3; whereas landslides in canyons and fjords can be smaller by several orders of magnitude (Fig. 15a) (Huhnerbach et al., 2004; Lee et al., 2007; Masson et al., 2006, 2002; Twichell et al., 2009). For example, in fjords, landslides commonly have volumes less than 1 km^3 (Fig. 15a). The size of landslides in fjords and canyons may be limited by the morphology of these geomorphic features (e.g. Syvitski et al. 1987; Huhnerbach et al. 2004). Continental slopes and the flanks of oceanic volcanic islands form very extensive submarine expanses with very little geomorphic variability, therefore, in the event that driving stresses prevail, they will likely act on large areas, producing large-scale failures (Masson et al., 2006).

Unexpectedly, along continental margins, most of the landslides occur in the outer slope, far from the shelf break, at water depths of ~1000 m or deeper (Fig. 15b) (Booth et al., 1993; Huhnerbach et al., 2004; McAdoo et al., 2000; Twichell et al., 2009) and along gentle slopes ranging between 3° and 4° (Fig. 15c) (Booth et al., 1993; Huhnerbach et al., 2004; Twichell et al., 2009). It has been reported that large landslides seem to preferentially occur on the lowest slopes, often as low as 1° (Fig. 15d) (Huhnerbach et al., 2004; McAdoo et al.,

2000). Statistical studies on the occurrence of landslides in different geological settings also suggest that there are fewer large landslides along active margins than along passive ones (Fig. 15e) (e.g. McAdoo et al. 2000; Camerlenghi et al. 2010).

Overall, the results of these statistical studies clearly indicate that slope and seismic loading alone are not important determining the location, occurrence and size of submarine landslides. Whereas a concurrence of multiple factors seems to be critical in controlling the origin and development of submarine slope failures (Camerlenghi et al., 2010; Lee et al., 2007; McAdoo et al., 2000; Twichell et al., 2009).

7   Concluding remarks

This chapter provides a summary of the classification schemes used to identify submarine landslides as well as the architectural elements that form them and the key factors that might control their emplacement in different geological environments. The contribution has shown that submarine landslides can occur in virtually every subaqueous settings, from fjords to canyon floors and to deepwater open slopes. A multitude of submarine slope processes can produce a highly variable occurrence of landslide deposits that exhibit a complex arrangement of internal structural styles characterising the headwall, translational and downslope domains. Future research will be critical to better understand how the interrelation of preconditioning and triggering factors control the initiation and emplacement of submarine landslides and how these might affect the resultant geomorphology of associated landslide deposits.
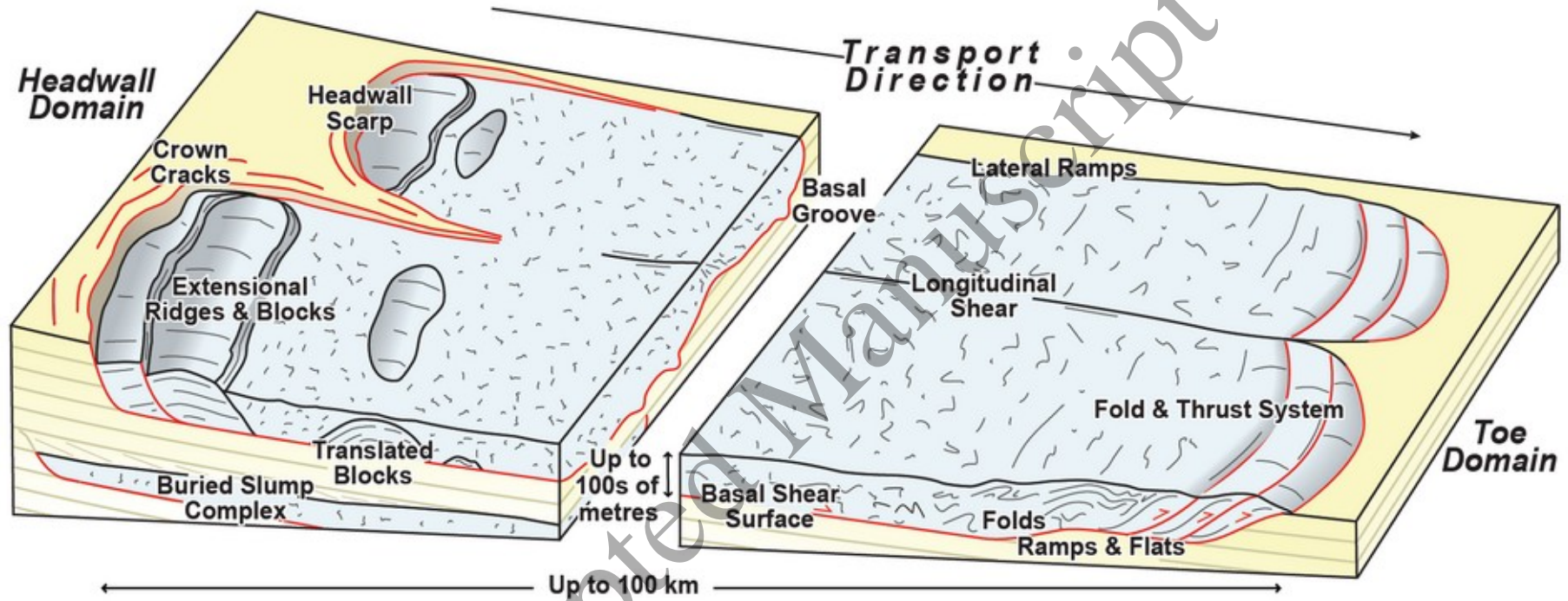
Figure 1: Schematic illustration of the morphology and structures of a submarine landslide. Compiled from Prior et al. (1984) and Bull et al. (2009).
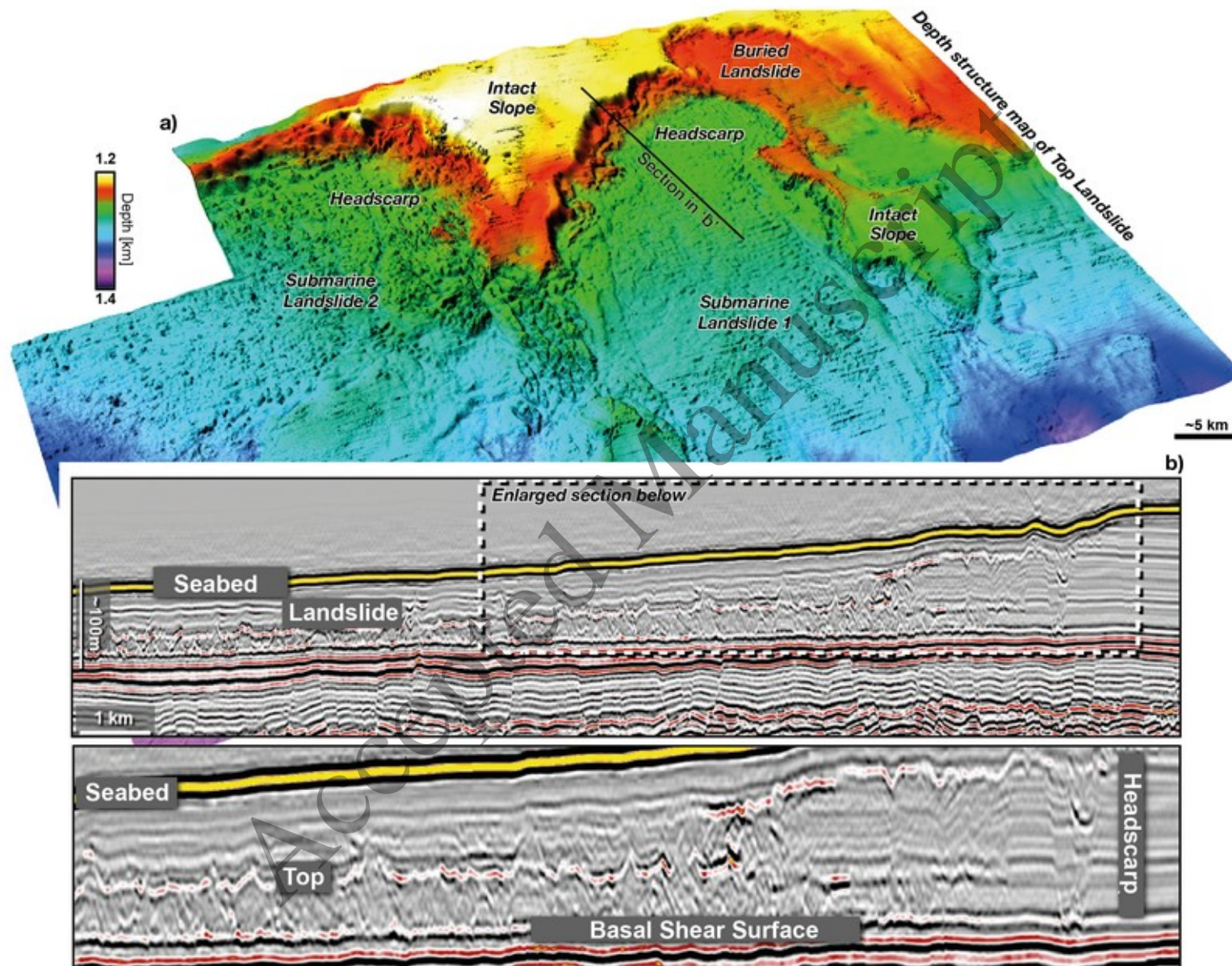
Figure 2: A typical example of submarine landslide as observed in reflection seismic data. a) Top surface map of the failure. b) Vertical section through the failure.
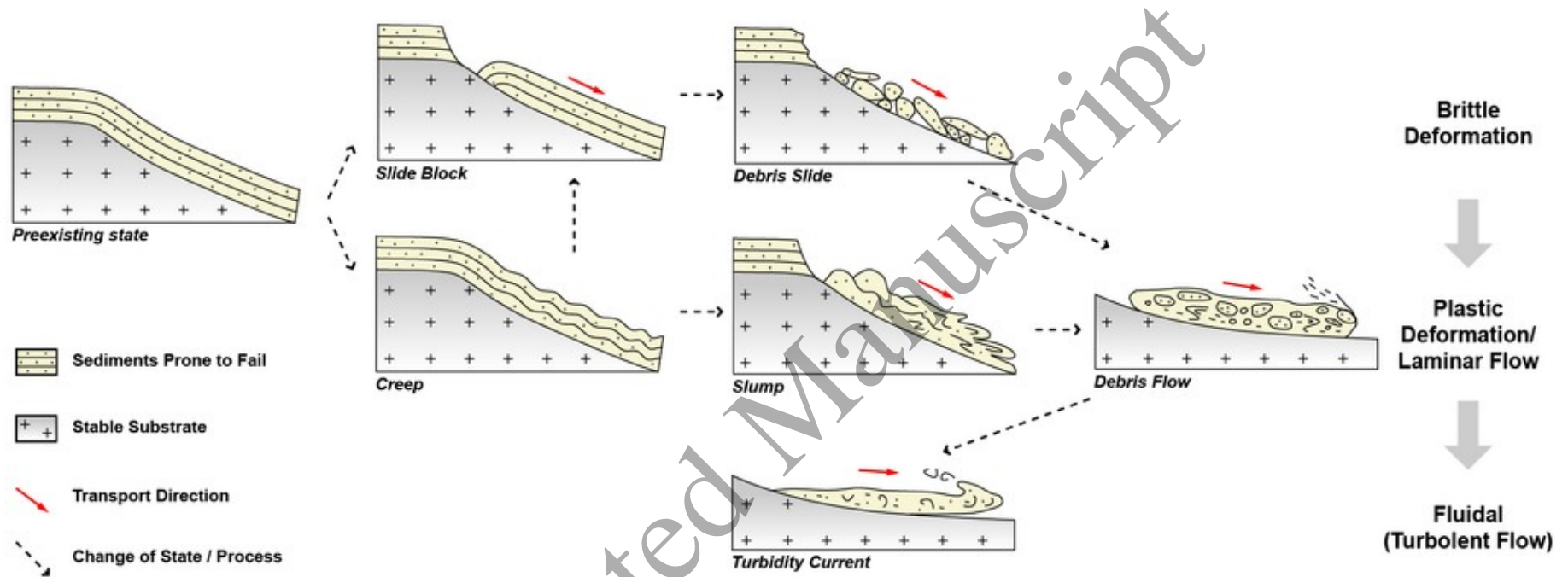
Figure 3: Summary of end member types of submarine mass movements. Modified from McHugh et al. (2002) and Madof er al. (2009).
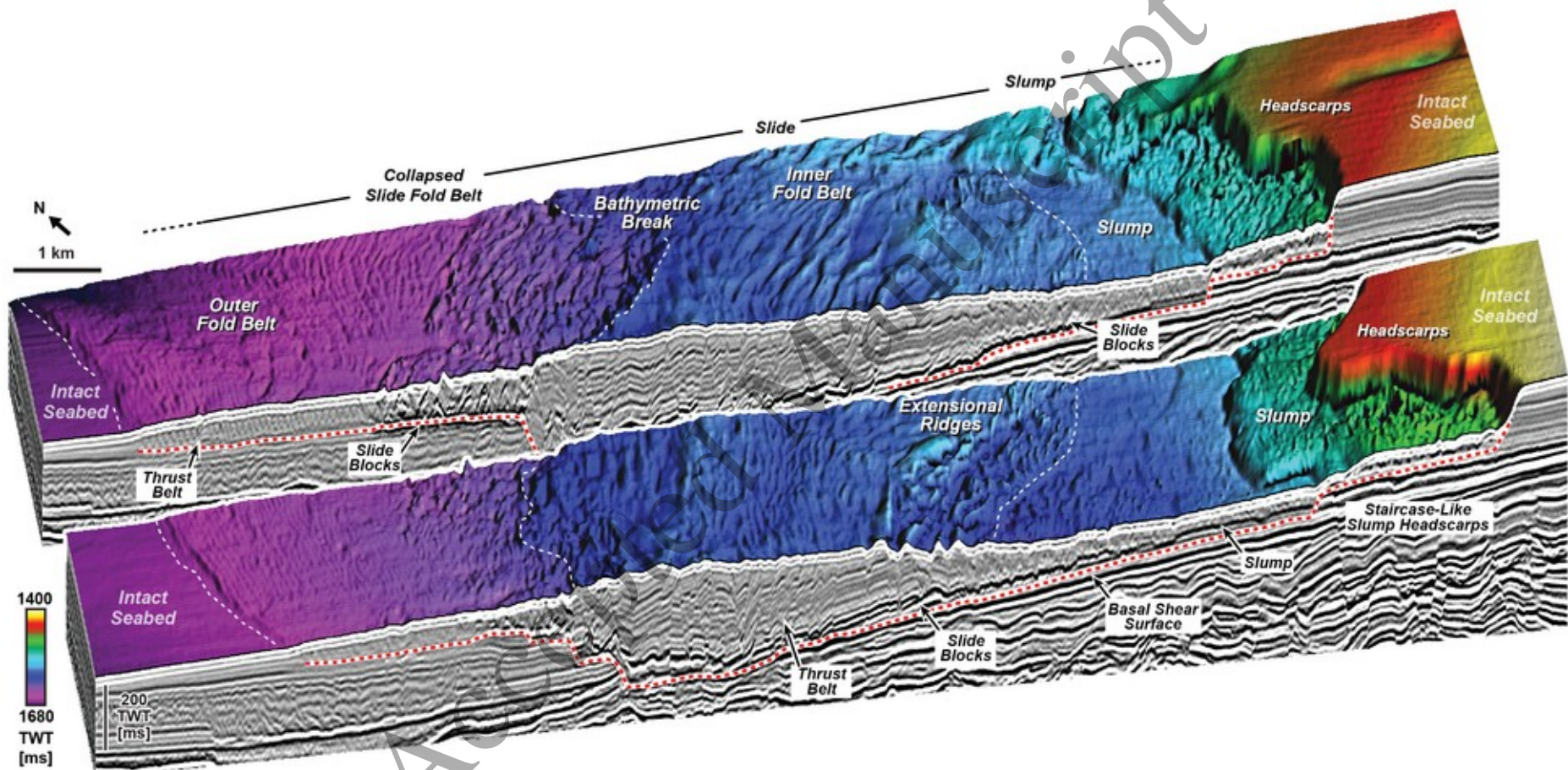
Figure 4: Seismic example of submarine landslide in which multiple failure processes coexist in the same event. The figure shows a recent, near seabed failure offshore NW Shelf Australia, where the headwall area is filled by a slump mass. This passes downslope to a coherent slide. Image from Scarselli et al. (2013).
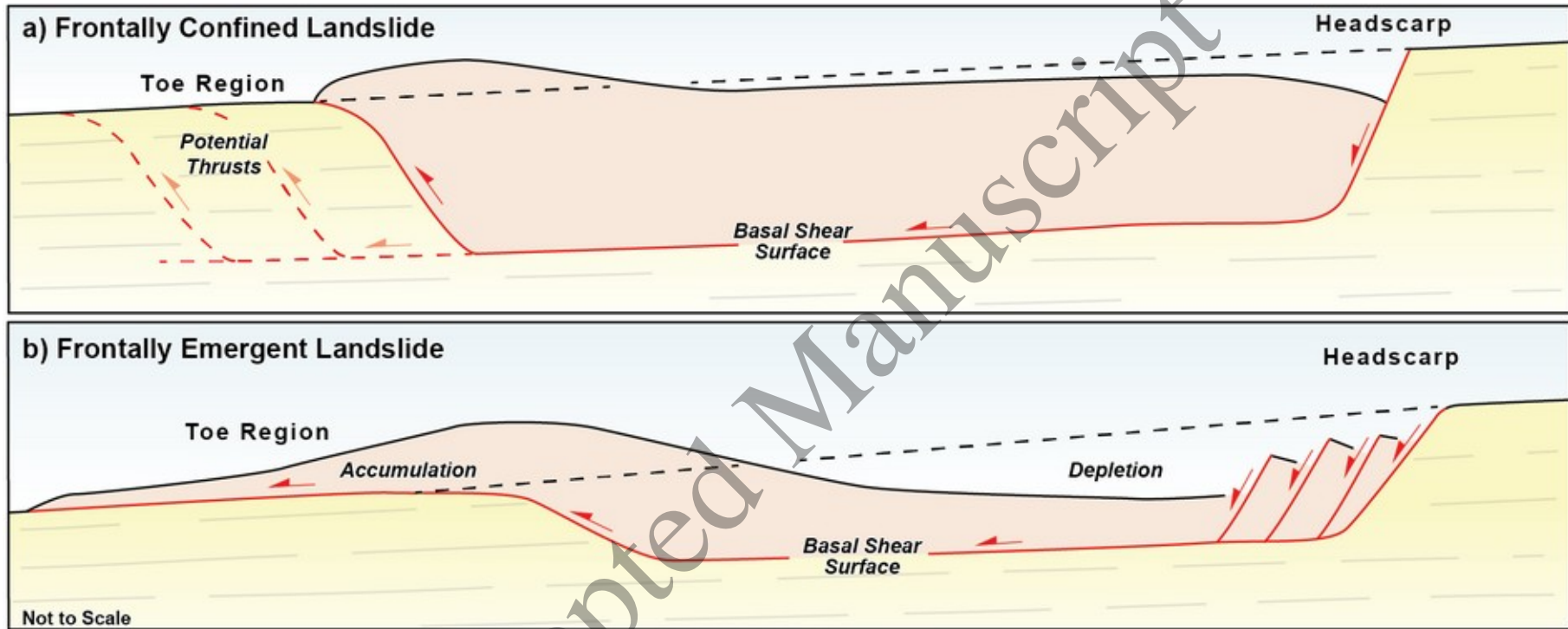
Figure 5: Schematic diagram of the classification of submarine landslides according to their frontal emplacement. a) Frontally confined landslides abut against a frontal ramp and do not abandon their basal shear surface. b) Frontally emergent landslides ramp up their basal shear surface and overrun the adjacent undeformed downslope strata. Modified from Frey-Martínez et al. (2006).
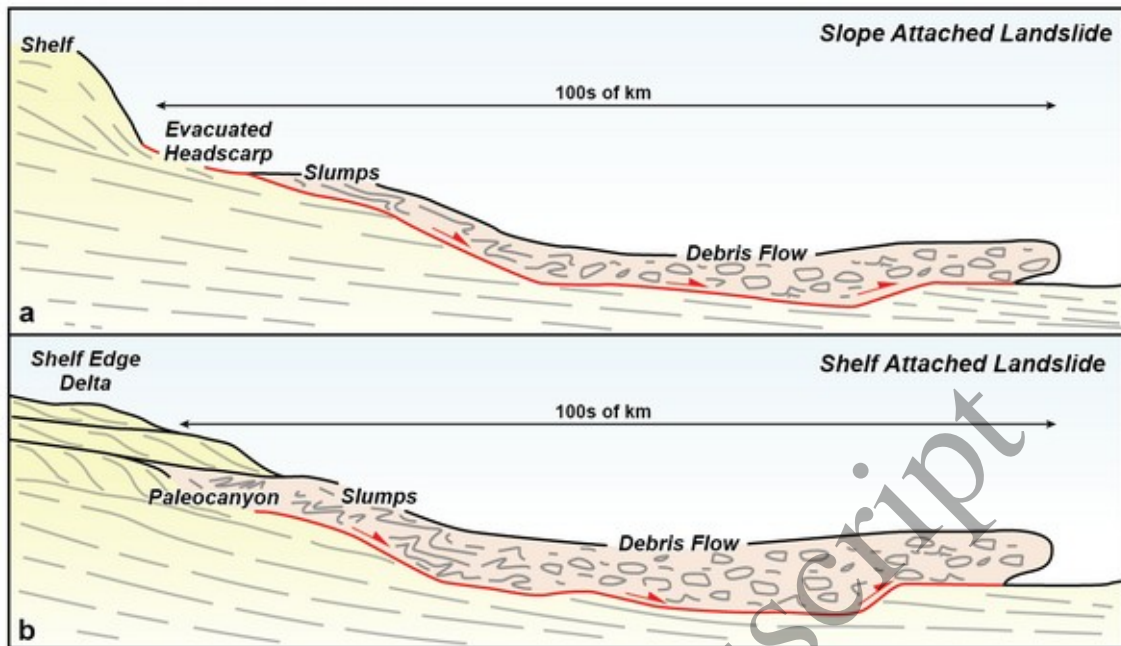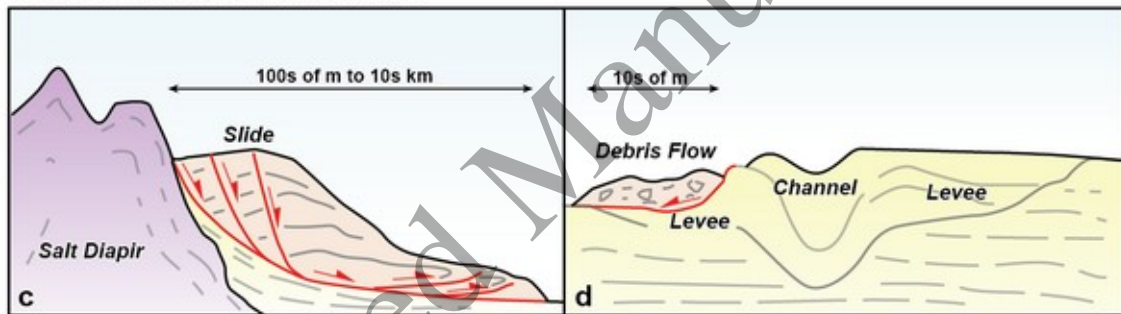
Figure 6: Schematic illustrations of attached and detached landslides. a) Slope attached landslides have their source region in the slope portion of the margin. b) Shelf-attached landslides result from the failure of shelf-edge deltas. c) Detached landslide created by the collapse of steep strata at the flanks of a salt diapir. d) Detached landslide originating from the steep flanks of a channel-levee complex. Modified from Moscardelli and Wood (2008).
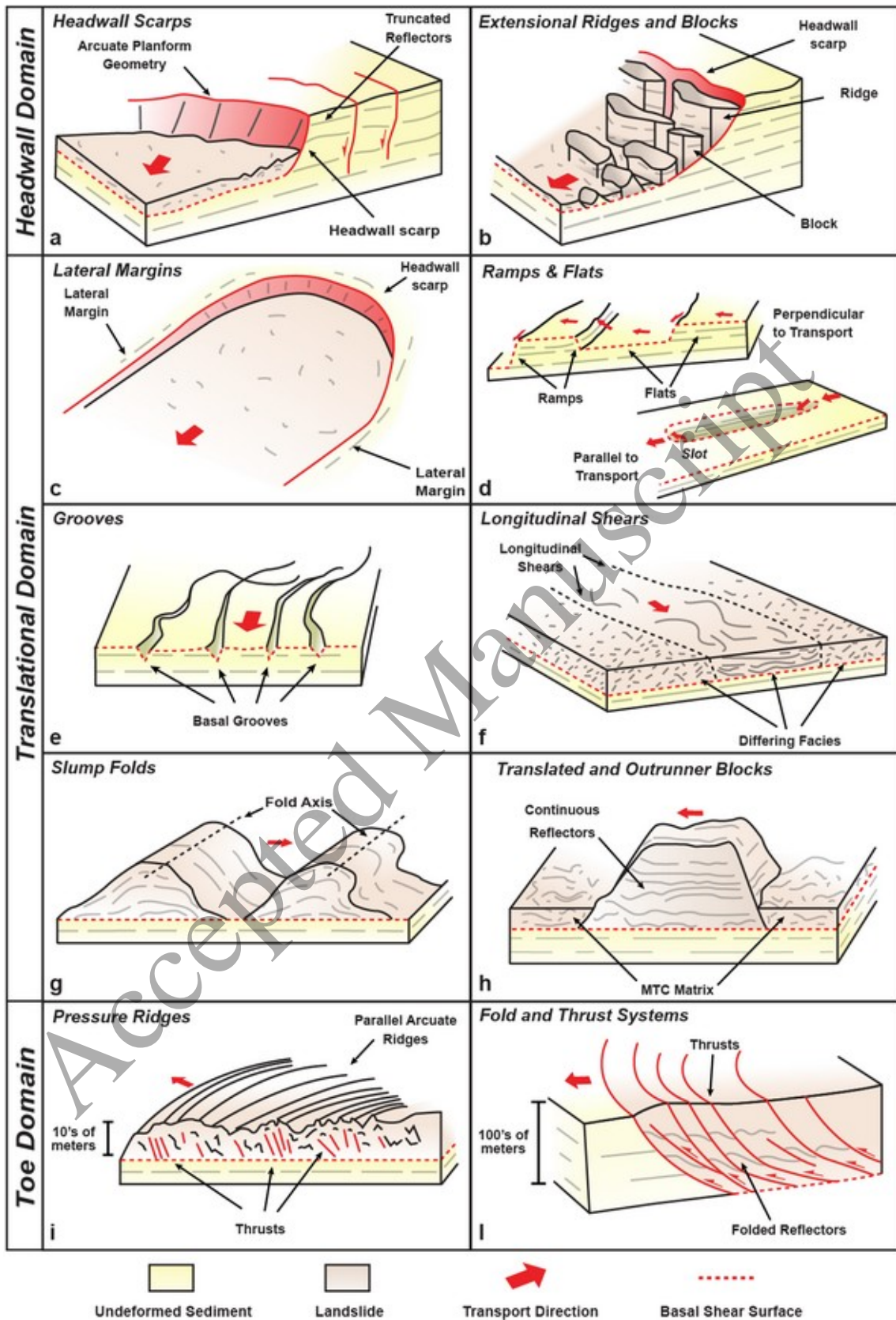
Figure 7: Summary of the main structures of submarine landslides. The structures are grouped according to the domain in which are likely to occur. Modified from Bull et al. (2009).
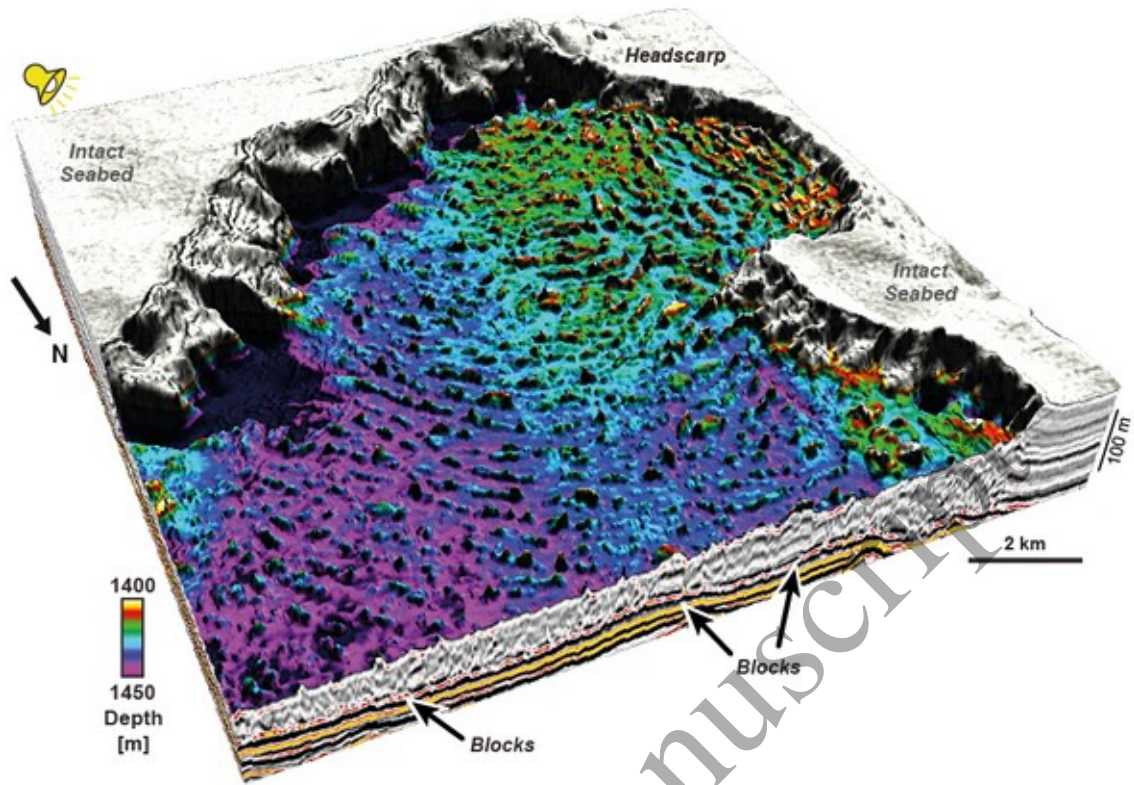
Figure 8: Extensional blocks at the headwall of submarine landslides. From Scarselli et al. 2020.
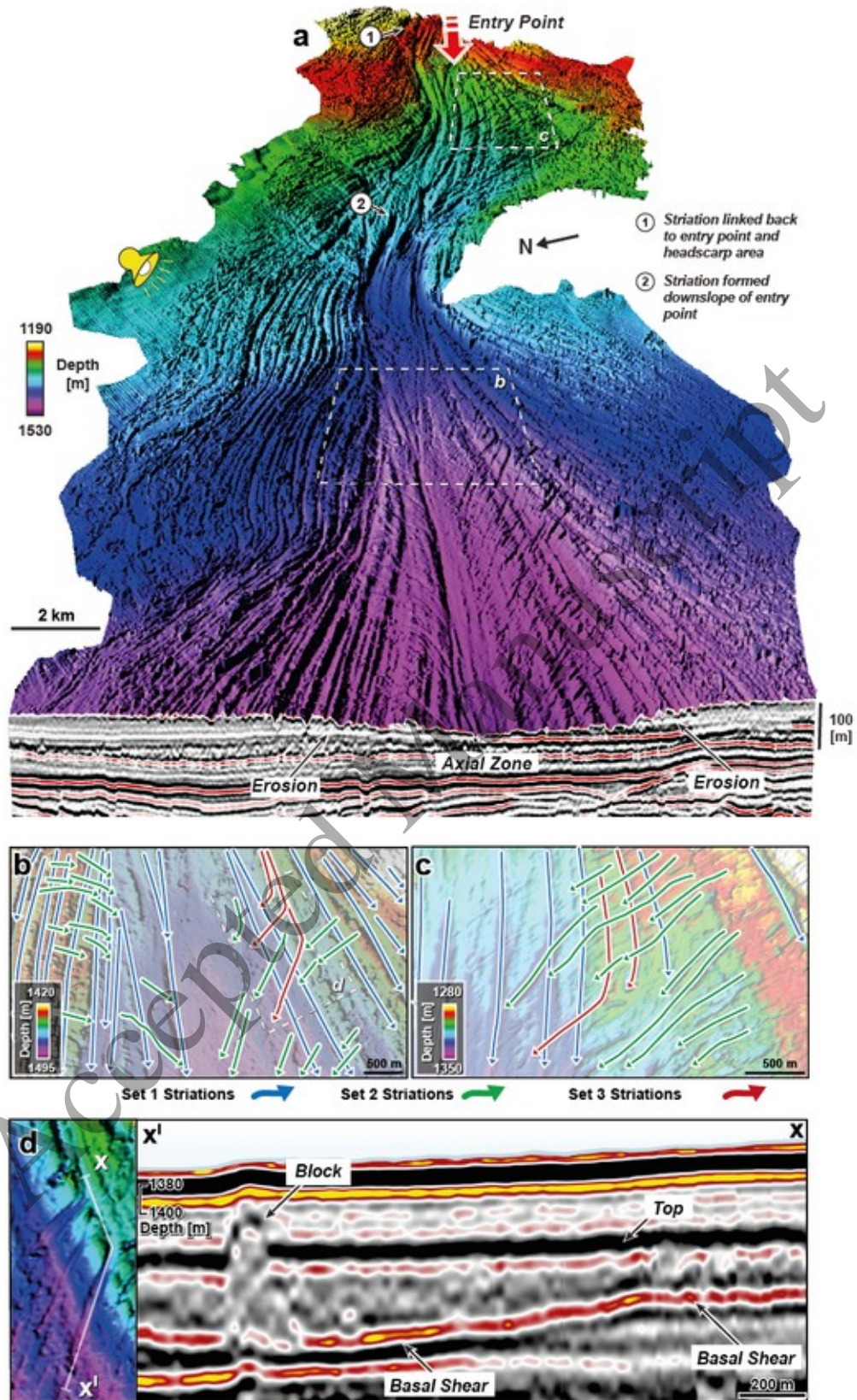
Figure 9: Example of striations at the base of a recent submarine landslide from the NW Shelf of Australia. a) Structure map of the basal shear surface showing clear striation originating from the headwall area. b & c) Detailed map views of the basal shear surface showing sets of striations with different orientation, indicating a complex transport within the failing mass (e.g. Scarselli et al 2013). d) longitudinal section across a striation showing that these are formed by a frontal block scouring the base of the slump mass.
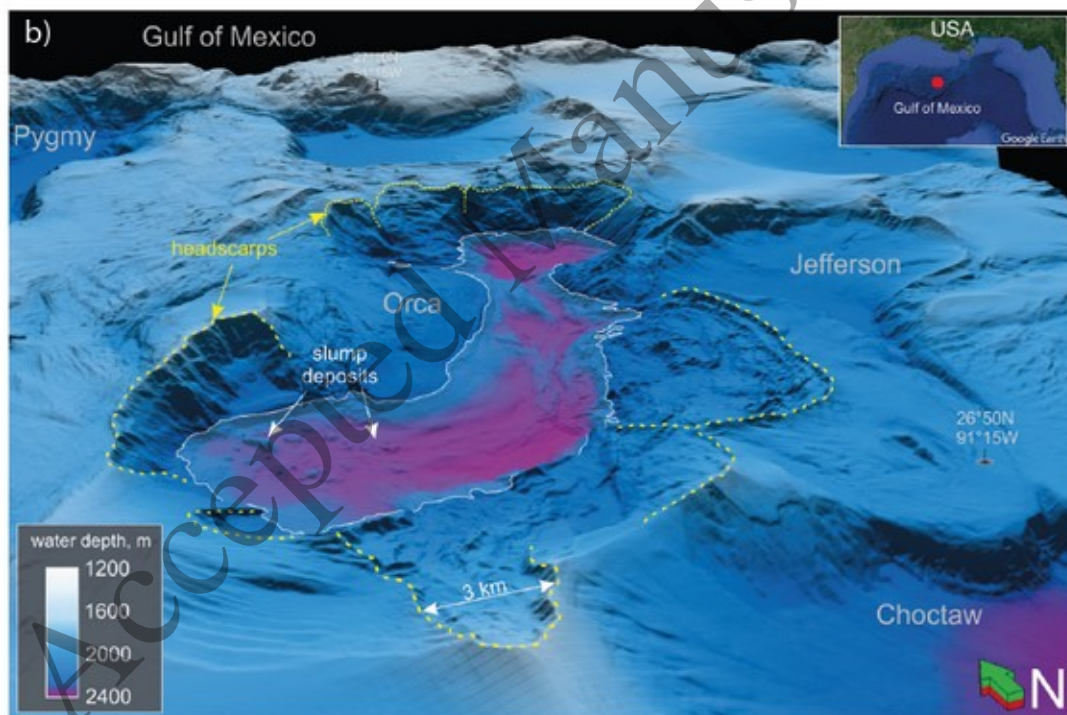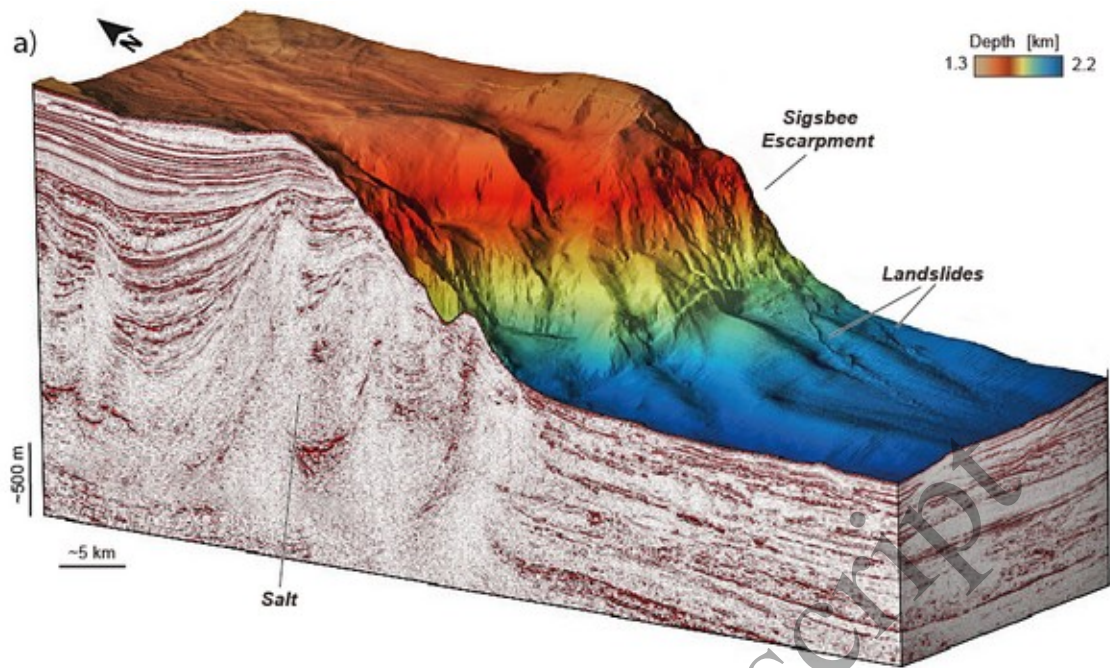
Figure 10: a) Three-dimensional view of seismic data and bathymetry of the eastern part of the Sigsbee Escarpment, Gulf of Mexico. The image shows the bathymetric relief of the Sigsbee Escarpment controlled by salt structures. The relief is affected by prominent erosion, in part related to the collapse of submarine landslides that are observed at the base of the escarpment. Image from Maselli & Kneller (2018). b) Three-dimensional view of bathymetric data depicting the Orca salt basin in the Gulf of Mexico. The image shows a number of landslide headscarps affecting the shoulders of the salt basins. Slump deposits are observed down dip from headscarps, in the deep part of the basin.Image from Sawyer at al. (2019).
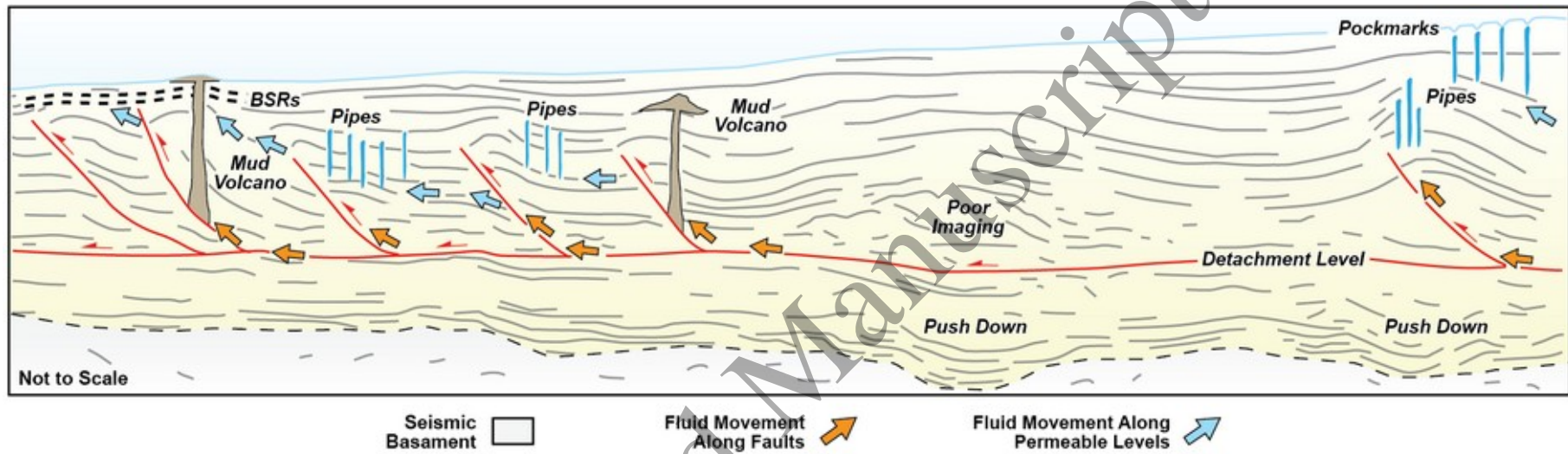
Figure 11: Schematic geoseismic section showing seismic indicators of fluid flow and ovepressures . Compiled from Rowan et al. (2004) and Morley et al. (2011).
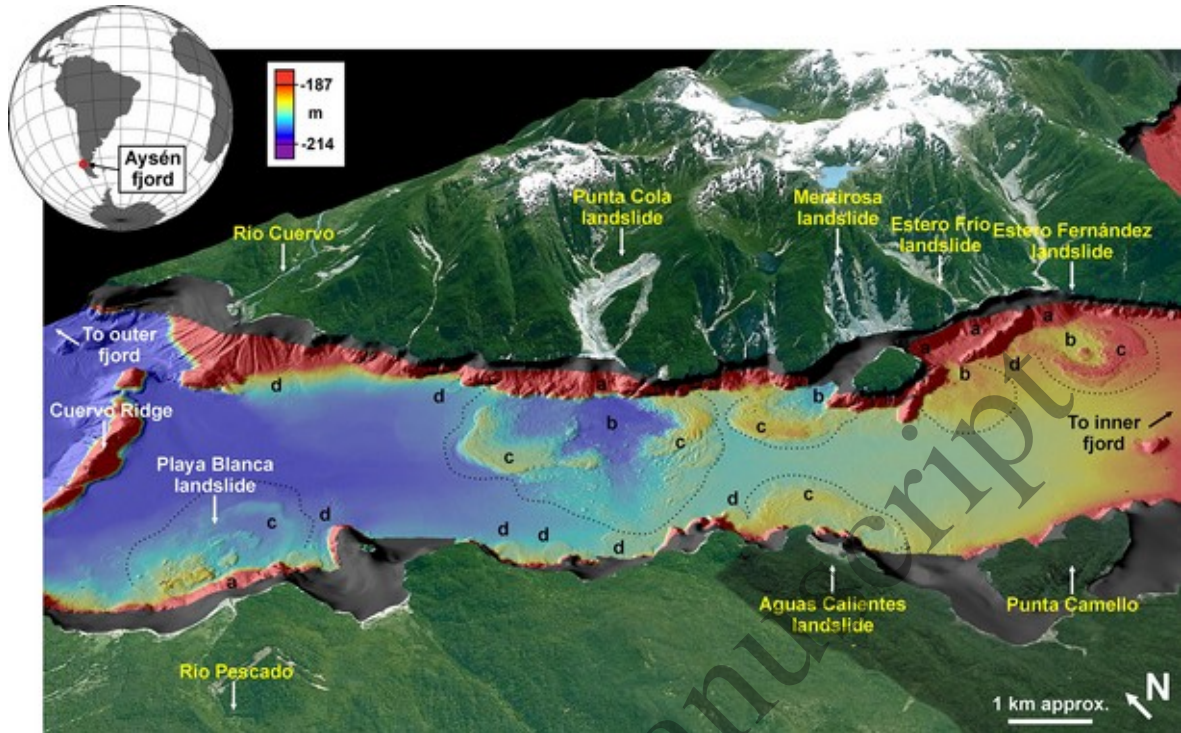
Figure 12: Digital elevation model and bathymetric data from the Aysen Fjord, Chile. The image shows a series of submarine landslides at the seabed, some appear to be linked, and perhaps triggered, by subaerial failures. Image from Lastras et al. (2013).
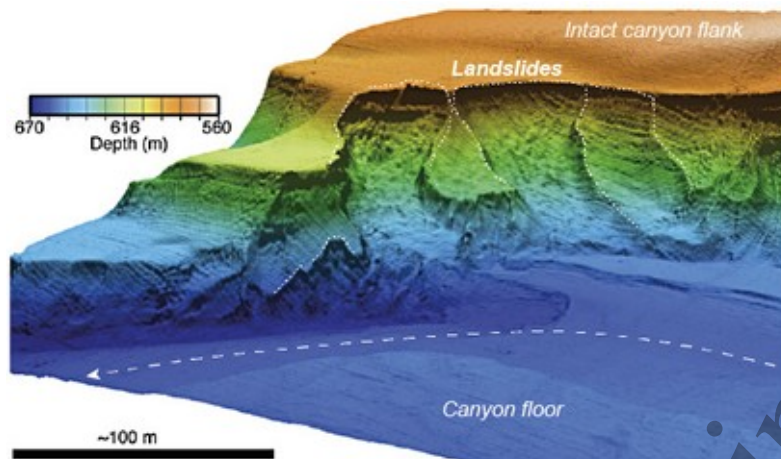
Figure 13: Submarine landslides affecting the northern flank of the La Jolla subamarine canyon, offshore California. Image from Paull et al. (2013).
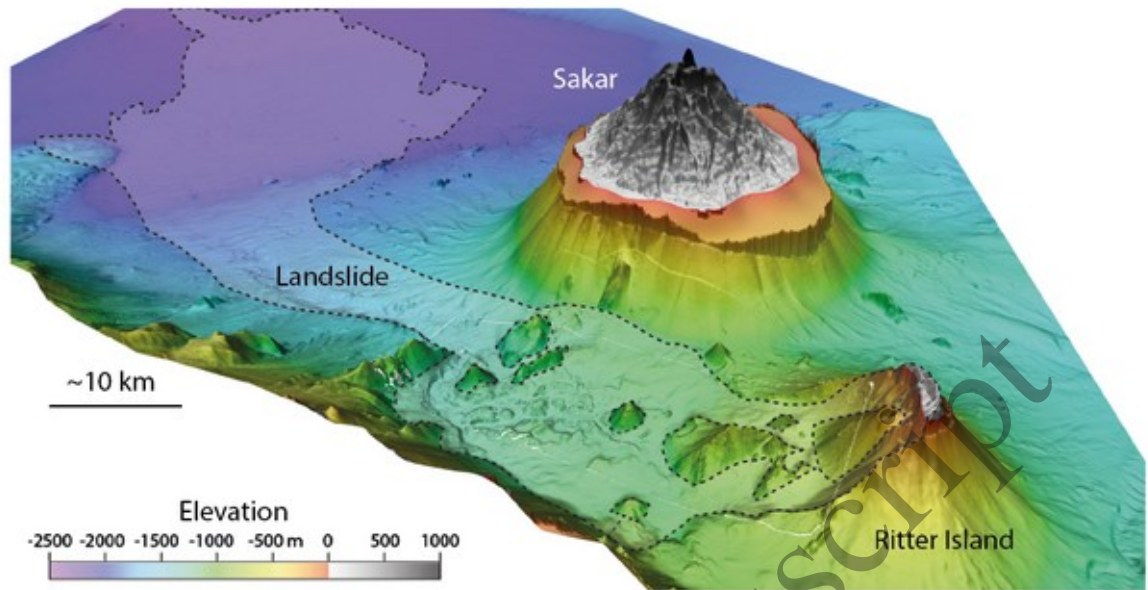
Figure 14: Digital elevation model showing the submarine landslide associated to the flank collapse of the Ritter Island volcano offshore north-east of New Guinea . Image from Karstens et al. (2019).

		Factors Causing Slope Instability	Environments and Geological Settings
Increasing Stress	*Slope Steepening*	Faulting, Folding and Diapirism	Passive and Active Margins, Salt Provinces
		Sediment Accumulation	Continental Slopes, Deltas, Fjords
		Erosion	Continental Slopes and Canyons
	Seismic Shaking	Earthquakes	Active Margins, Glaciated Margins, Fjords, (Passive Margins)
	Wave Loading	Hurricanes	Deltas and Continentals Shelves (water depth < 100m)
		Tsunamis	
		Storms	
Reducing Strength	*Excess Pore Fluid Pressure*	Dissociation of Gas Hydrate	Continental Slopes (water depth < 500m)
		Decay of Organic Matter	Deltas, Fjords
		Fluid Seepage and Migration	Fjords, Continental Slopes
		Earthquakes	Active Margins, Glaciated Margins, Fjords, (Passive Margins)
		High Sedimentation Rate	Fjords, Deltas and Continental Slopes

Triggering Factor   Preconditioning Factor

Table 1: Causes of submarine slope failure and environments where they are likely to have relevance in causing landslides. Compiled from Hampton et al. (1996); McAdoo et al. (2000); Locat and Lee (2002); Judd and Hovland (2007); Lee et al. (2007).
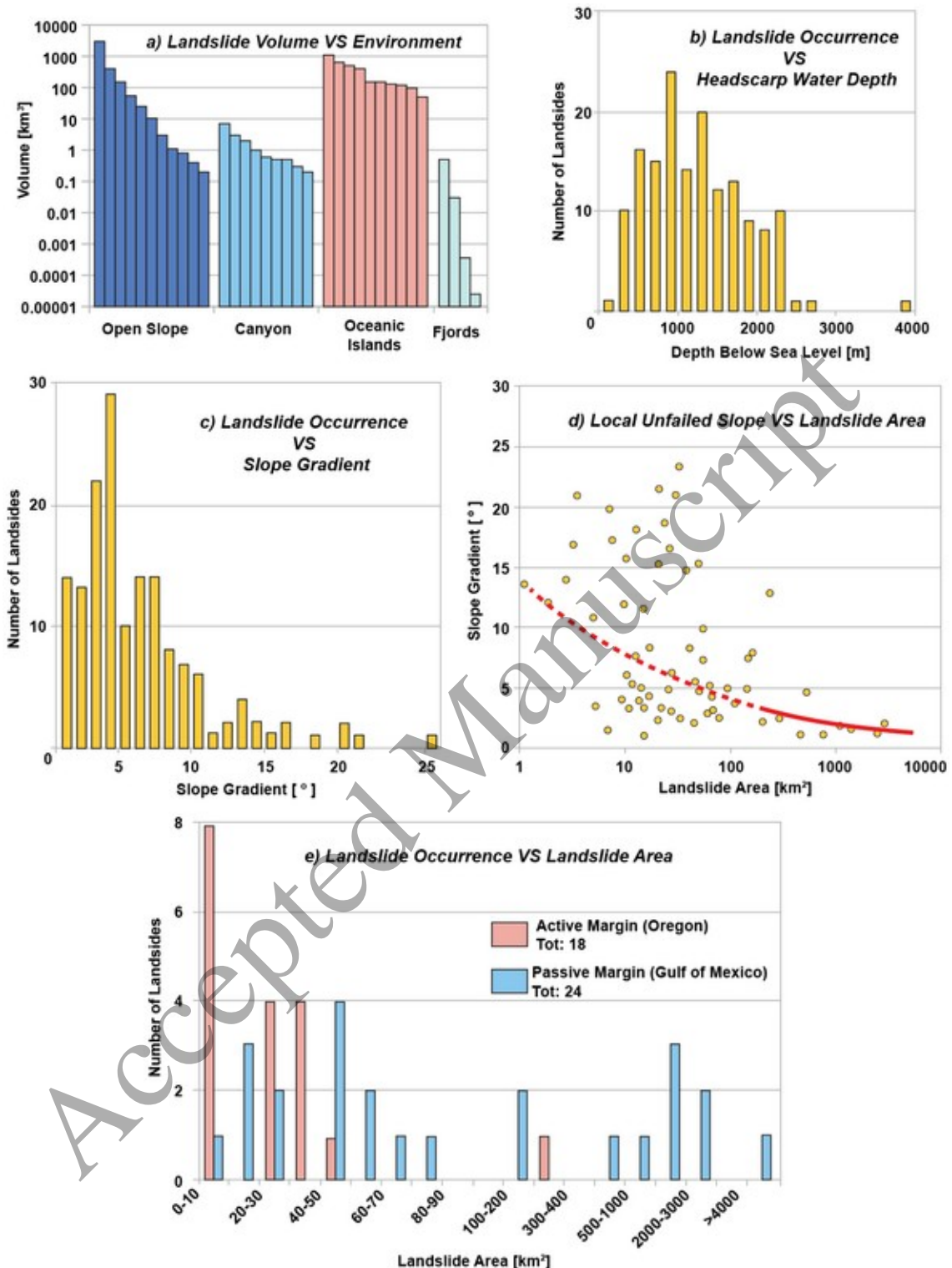
Figure 15: a) Range of volumes for landslides in different environments. Largest landslides occur in open continental slopes and oceanic volcanic islands. Compiled from Masson et al. (2002); Twichell et al. (2009); Stoker et al. (2010); b) Occurrence of landslides at different water depth. Most of the landslides originate at water depth of ~1000m. Modified from Huhnerbach et al. (2004). c) Occurrence of landslide at different slope gradients. Landslide occurs mostly on gentle slopes ~ 3°. Modified from Huhnerbach et al. (2004). d) Slope gradient plotted against landslide area. The largest landslides occur on gentle slope < 5°. Modified from McAdoo et al. (2000). e) Occurrence of landslides plotted against the total landslides area for the active margin of Oregon and the passive margin of the Gulf of Mexico. Large landslides do not necessarily occur in seismically active regions. Modified from McAdoo et al. (2000).

Alexander, C.R., DeMaster, D.J., Nittrouer, C.A., 1991. Sediment accumulation in a modern epicontinental-shelf setting: the Yellow Sea. Marine Geology 98, 51–72.

Alsop, G.I., Marco, S., 2014. Fold and fabric relationships in temporally and spatially evolving slump systems: A multi-cell flow model. Journal of Structural Geology 63, 27–49. https://doi.org/10.1016/j.jsg.2014.02.007

Alsop, G.I., Marco, S., Levi, T., Weinberger, R., 2017. Fold and thrust systems in Mass Transport Deposits. Journal of Structural Geology 94, 98–115. https://doi.org/10.1016/j.jsg.2016.11.008

Alsop, G.I., Weinberger, R., Marco, S., Levi, T., 2019. Fold and Thrust Systems in Mass-Transport Deposits Around the Dead Sea Basin, in: Ogata, K., Festa, A., Pini, G.A. (Eds.), Geophysical Monograph Series. Wiley, pp. 139–153. https://doi.org/10.1002/9781119500513.ch9

Alves, T.M., Lourenco, S.D.N., 2010. Geomorphologic features related to gravitational collapse: Submarine landsliding to lateral spreading on a Late Miocene-Quaternary slope (SE Crete, eastern Mediterranean). Geomorphology 123, 13–33.

Antobreh, A.A., Krastel, S., 2006. Morphology, seismic characteristics and development of Cap Timiris Canyon, offshore Mauritania: a newly discovered canyon preserved-off a major arid climatic region. Marine and petroleum geology 23, 37–59.

Bea, R.G., Sircar, P., Niedoroda, A.W., 1983. Wave-Induced Slides in South Pass Block 70, Mississippi Delta. Journal of Geotechnical Engineering 109, 619.

Bertoni, C., Cartwright, J., 2005. 3D seismic analysis of slope-confined canyons from the Plio–Pleistocene of the Ebro Continental Margin (Western Mediterranean). Basin Research 17, 43–62.

Biscontin, G., Pestana, J.M., Nadim, F., 2004. Seismic triggering of submarine slides in soft cohesive soil deposits. Marine Geology 203, 341–354. https://doi.org/10.1016/S0025-3227(03)00314-1

Booth, J.S., O'Leary, D.W., Popenoe, P., Danforth, W.W., 1993. US Atlantic continental slope landslides: their distribution, general attributes, and implications. Submarine Landslides: Selected Studies in the US Exclusive Economic Zone 14–22.

Bornhold, B.D., Prior, D.B., 1989. Sediment blocks on the sea floor in British Columbia fjords. Geo-Marine Letters 9, 135–144. https://doi.org/10.1007/BF02431040

Boulanger, É., 2000. Comportement cyclique des sédiments de la marge continentale de la rivière Eel, une explication possible pour le peu de glissements sous-marins superficiels dans cette région.

Boulanger, E., Konrad, J.M., Locat, J., Lee, H.J., 1998. Cyclic behavior of Eel River sediments: a possible explanation for the paucity of submarine landslide features. American Geophysical Union San Francisco, in: EOS, Abstract. p. 254.

Bradley, D., Hanson, L., 1998. Paleoslope Analysis of Slump Folds in the Devonian Flysch of Maine. J GEOL 106, 305–318. https://doi.org/10.1086/516024

Bull, S., Cartwright, J., Huuse, M., 2009. A review of kinematic indicators from mass-transport complexes using 3D seismic data. Marine and Petroleum Geology 26, 1132–1151. https://doi.org/10.1016/j.marpetgeo.2008.09.011

Butler, R.W.H., McCaffrey, W.D., 2010. Structural evolution and sediment

entrainment in mass-transport complexes: outcrop studies from Italy. Journal of the Geological Society 167, 617.

Butler, R.W.H., Turner, J.P., 2010. Gravitational collapse at continental margins: products and processes; an introduction. Journal of the Geological Society 167, 569–570. https://doi.org/10.1144/0016-76492010-003

Callot, P., Sempere, T., Odonne, F., Robert, E., 2008. Giant submarine collapse of a carbonate platform at the Turonian-Coniacian transition: The Ayabacas Formation, southern Peru. Basin Research 20, 333–357. https://doi.org/10.1111/j.1365-2117.2008.00358.x

Camerlenghi, A., Urgeles, R., Fantoni, L., 2010. A Database on Submarine Landslides of the Mediterranean Sea. Submarine Mass Movements and Their Consequences 503–513.

Canals, M., Lastras, G., Urgeles, R., Casamor, J.L., Mienert, J., Cattaneo, A., De Batist, M., Haflidason, H., Imbo, Y., Laberg, J.S., Locat, J., Long, D., Longva, O., Masson, D.G., Sultan, N., Trincardi, F., Bryn, P., 2004. Slope failure dynamics and impacts from seafloor and shallow sub-seafloor geophysical data: case studies from the COSTA project. Marine Geology 213, 9–72. https://doi.org/10.1016/j.margeo.2004.10.001

Chadwick, W. w., Dziak, R. p., Haxel, J. h., Embley, R. w., Matsumoto, H., 2012. Submarine landslide triggered by volcanic eruption recorded by in situ hydrophone. Geology 40, 51–54. https://doi.org/10.1130/G32495.1

Chaytor, J.D., ten Brink, U.S., Solow, A.R., Andrews, B.D., 2009. Size distribution of submarine landslides along the US Atlantic margin. Marine Geology 264, 16–27.

Coleman, J.M., 1976. Deltas: processes of deposition & models for exploration. Continuing Education Publication Co., Champaign, Ill.

Counts, J.W., Jorry, S.J., Leroux, E., Miramontes, E., Jouet, G., 2018. Sedimentation adjacent to atolls and volcano-cored carbonate platforms in the Mozambique Channel (SW Indian Ocean). Marine Geology 404, 41–59. https://doi.org/10.1016/j.margeo.2018.07.003

Cunningham, M.J., Hodgson, S., Masson, D.G., Parson, L.M., 2005. An evaluation of along- and down-slope sediment transport processes between Goban Spur and Brenot Spur on the Celtic Margin of the Bay of Biscay. Sedimentary Geology 179, 99–116. https://doi.org/10.1016/j.sedgeo.2005.04.014

Davie, M.K., Buffett, B.A., 2003. Sources of methane for marine gas hydrate: inferences from a comparison of observations and numerical models. Earth and Planetary Science Letters 206, 51–63. https://doi.org/10.1016/S0012-821X(02)01064-6

Dingle, R.V., 1980. Large allochthonous sediment masses and their role in the construction of the continental slope and rise off southwestern Africa. Marine Geology 37, 333–354. https://doi.org/10.1016/0025-3227(80)90109-7

Dugan, B., Flemings, P.B., 2002. Fluid flow and stability of the US continental slope offshore New Jersey from the Pleistocene to the present. Geofluids 2, 137–146.

Dugan, B., Flemings, P.B., 2000. Overpressure and fluid flow in the New Jersey continental slope: Implications for slope failure and cold seeps. Science 289, 288.

Ellis, S., Pecher, I., Kukowski, N., Xu, W., Henrys, S., Greinert, J., 2010. Testing proposed mechanisms for seafloor weakening at the top of gas hydrate

stability on an uplifted submarine ridge (Rock Garden), New Zealand. Marine Geology 272, 127–140. https://doi.org/10.1016/j.margeo.2009.10.008

Embley, R.W., Jacobi, R.D., 1977. Distribution and morphology of large submarine sediment slides and slumps on Atlantic continental margins. Marine Georesources & Geotechnology 2, 205–228.

Farmer, D.M., Freeland, H.J., 1983. The physical oceanography of fjords. Progress in oceanography 12, 147–220.

Farrell, S.G., Eaton, S., 1987. Slump strain in the Tertiary of Cyprus and the Spanish Pyrenees. Definition of palaeoslopes and models of soft-sediment deformation. Geological Society, London, Special Publications 29, 181–196. https://doi.org/10.1144/GSL.SP.1987.029.01.15

Felix, M., Peakall, J., 2006. Transformation of debris flows into turbidity currents: mechanisms inferred from laboratory experiments. Sedimentology 53, 107–123.

Fleischer, P., Orsi, T., Richardson, M., Anderson, A., 2001. Distribution of free gas in marine sediments: a global overview. Geo-Marine Letters 21, 103–122.

Flemings, P.B., Long, H., Dugan, B., Germaine, J., John, C.M., Behrmann, J.H., Sawyer, D., IODP, E., others, 2008. Pore pressure penetrometers document high overpressure near the seafloor where multiple submarine landslides have occurred on the continental slope, offshore Louisiana, Gulf of Mexico. Earth and Planetary Science Letters 269, 309–325.

Floodgate, G.D., Judd, A.G., 1992. The origins of shallow gas. Continental Shelf Research 12, 1145–1156. https://doi.org/10.1016/0278-4343(92)90075-U

Frey-Martínez, J., 2010. 3D Seismic Interpretation of Mass Transport Deposits: Implications for Basin Analysis and Geohazard Evaluation. Submarine Mass Movements and Their Consequences 553–568.

Frey-Martínez, J. [1], Cartwright, J. [1], Hall, B. [2], 2005. 3D seismic interpretation of slump complexes: examples from the continental margin of Israel. Basin Research 17, 83–108. https://doi.org/10.1111/j.1365-2117.2005.00255.x

Frey-Martínez, J., Cartwright, J., James, D., 2006. Frontally confined versus frontally emergent submarine landslides: A 3D seismic characterisation. Marine and Petroleum Geology 23, 585–604. https://doi.org/10.1016/j.marpetgeo.2006.04.002

Gafeira, J., Long, D., Scrutton, R., Evans, D., 2010. 3D seismic evidence of internal structure within Tampen Slide deposits on the North Sea Fan: are chaotic deposits that chaotic? Journal of the Geological Society 167, 605–616. https://doi.org/<p>10.1144/0016-76492009-047</p>

García-Tortosa, F.J., Alfaro, P., Gibert, L., Scott, G., 2011. Seismically induced slump on an extremely gentle slope (< 1°) of the Pleistocene Tecopa paleolake (California). Geology.

Gavey, R., Carter, L., Liu, J.T., Talling, P.J., Hsu, R., Pope, E., Evans, G., 2017. Frequent sediment density flows during 2006 to 2015, triggered by competing seismic and weather events: Observations from subsea cable breaks off southern Taiwan. Marine Geology 384, 147–158. https://doi.org/10.1016/j.margeo.2016.06.001

Gee, M.J.R., Gawthorpe, R.L., Friedmann, S.J., 2006. Triggering and evolution of a giant submarine landslide, offshore Angola, revealed by 3D seismic stratigraphy and geomorphology. Journal of Sedimentary Research 76,

9–19.

Gee, M.J.R., Uy, H.S., Warren, J., Morley, C.K., Lambiase, J.J., 2007. The Brunei slide: A giant submarine landslide on the North West Borneo Margin revealed by 3D seismic data. Marine Geology 246, 9–23. https://doi.org/10.1016/j.margeo.2007.07.009

Hampton, M.A., Lee, H.J., Locat, J., 1996. Submarine Landslides. Reviews of Geophysics 34, 33–59.

He, Y., Zhong, G., Wang, L., Kuang, Z., 2014. Characteristics and occurrence of submarine canyon-associated landslides in the middle of the northern continental slope, South China Sea. Marine and Petroleum Geology 57, 546–560. https://doi.org/10.1016/j.marpetgeo.2014.07.003

Henkel, D.J., 1970. The role of waves in causing submarine landslides. Geotechnique 20, 75–80.

Horozal, S., Bahk, J.-J., Urgeles, R., Kim, G.Y., Cukur, D., Kim, S.-P., Lee, G.H., Lee, S.H., Ryu, B.-J., Kim, J.-H., 2017. Mapping gas hydrate and fluid flow indicators and modeling gas hydrate stability zone (GHSZ) in the Ulleung Basin, East (Japan) Sea: Potential linkage between the occurrence of mass failures and gas hydrate dissociation. Marine and Petroleum Geology 80, 171–191. https://doi.org/10.1016/j.marpetgeo.2016.12.001

Huhnerbach, V., Masson, D.G., others, 2004. Landslides in the North Atlantic and its adjacent seas: an analysis of their morphology, setting and behaviour. Marine geology 213, 343–362.

Hürlimann, M., Garcia-Piera, J.O., Ledesma, A., 2000. Causes and mobility of large volcanic landslides: application to Tenerife, Canary Islands. Journal of volcanology and geothermal research 103, 121–134.

Huuse, M., Jackson, C.A.-L., Van Rensbergen, P., Davies, R.J., Flemings, P.B., Dixon, R.J., 2010. Subsurface sediment remobilization and fluid flow in sedimentary basins: an overview. Basin Research 22, 342–360. https://doi.org/10.1111/j.1365-2117.2010.00488.x

Ireland, M.T., Davies, R.J., Goulty, N.R., Moy, D.J., 2011. Thick slides dominated by regular-wavelength folds and thrusts in biosiliceous sediments on the Vema Dome offshore of Norway. Marine Geology In Press, Accepted Manuscript. https://doi.org/10.1016/j.margeo.2011.08.001

Iverson, R.M., 1997. The physics of debris flows. Reviews of Geophysics 35, 245–296.

Jackson, C.A.-L., 2011. Three-dimensional seismic analysis of megaclast deformation within a mass transport deposit; implications for debris flow kinematics. Geology 39, 203–206. https://doi.org/10.1130/G31767.1

Jeng, D.S., 2003. Wave-induced sea floor dynamics. Applied Mechanics Reviews 56, 407.

Jeng, D.S., 2001. Mechanism of the wave-induced seabed instability in the vicinity of a breakwater: a review. Ocean Engineering 28, 537–570. https://doi.org/10.1016/S0029-8018(00)00013-5

Karstens, J., Berndt, C., Urlaub, M., Watt, S.F.L., Micallef, A., Ray, M., Klaucke, I., Muff, S., Klaeschen, D., Kühn, M., Roth, T., Böttner, C., Schramm, B., Elger, J., Brune, S., 2019. From gradual spreading to catastrophic collapse – Reconstruction of the 1888 Ritter Island volcanic sector collapse from high-resolution 3D seismic data. Earth and Planetary Science Letters 517, 1–13. https://doi.org/10.1016/j.epsl.2019.04.009

Katz, O., Reuven, E., Aharonov, E., 2015. Submarine landslides and fault scarps along the eastern Mediterranean Israeli continental-slope. Marine Geology 369, 100–115. https://doi.org/10.1016/j.margeo.2015.08.006

Kneller, B., Buckee, C., 2000. The structure and fluid mechanics of turbidity currents: a review of some recent studies and their geological implications. Sedimentology 47, 62–94.

Kopf, A.J., Kasten, S., Blees, J., 2010. Geochemical evidence for groundwater-charging of slope sediments: The Nice airport 1979 landslide and tsunami revisited. Submarine Mass Movements and Their Consequences 203–214.

Kuehl, S.A., Levy, B.M., Moore, W.S., Allison, M.A., 1997. Subaqueous delta of the Ganges-Brahmaputra river system. Marine Geology 144, 81–96.

Kvenvolden, K.A., 1993. Gas hydrates—geological perspective and global change. Rev. Geophys 31, 173–187.

Laberg, J.S., Camerlenghi, A., 2008. The significance of contourites for submarine slope stability. Developments in Sedimentology 60, 537–556.

Lastras, G., Amblas, D., Calafat, A.M., Canals, M., Frigola, J., Hermanns, R.L., Lafuerza, S., Longva, O., Micallef, A., Sepúlveda, S.A., Vargas, G., Batist, M.D., Daele, M.V., Azpiroz, M., Bascuñán, I., Duhart, P., Iglesias, O., Kempf, P., Rayo, X., 2013. Landslides Cause Tsunami Waves: Insights From Aysén Fjord, Chile. Eos Trans. AGU 94, 297–298. https://doi.org/10.1002/2013EO340002

Lastras, G., Arzola, R.G., Masson, D.G., Wynn, R.B., Huvenne, V.A.I., Hühnerbach, V., Canals, M., 2009. Geomorphology and sedimentary features in the Central Portuguese submarine canyons, Western Iberian margin. Geomorphology 103, 310–329. https://doi.org/10.1016/j.geomorph.2008.06.013

Lee, H.J., 2009. Timing of occurrence of large submarine landslides on the Atlantic Ocean margin. Marine Geology 264, 53–64.

Lee, H.J., Locat, J., Desgagnés, P., Parsons, J.D., McAdoo, B.G., Orange, D.L., Puig, P., Wong, F.L., Dartnell, P., Boulanger, E., 2007. Submarine Mass Movements on Continental Margins, in: Nittrouer, C.A., Austin, J.A., Field, M.E., Kravitz, J.H., Syvitski, J.P.M., Wiberg, P.L. (Eds.), Continental Margin Sedimentation: From Sediment Transport to Sequence Stratigraphy, Special Publication of the International Association Of Sedimentologists, 37. Wiley-Blackwell, pp. 213–274.

Leynaud, D., Mienert, J., Vanneste, M., 2009. Submarine mass movements on glaciated and non-glaciated European continental margins: A review of triggering mechanisms and preconditions to failure. Marine and Petroleum Geology 26, 618–632.

Locat, J., Lee, H.J., 2002. Submarine landslides: advances and challenges. Canadian Geotechnical Journal 39, 193–212.

Lucente, C.C., Pini, G.A., 2008. Basin-wide mass-wasting complexes as markers of the Oligo-Miocene foredeep-accretionary wedge evolution in the Northern Apennines, Italy. Basin Research 20, 49–71. https://doi.org/10.1111/j.1365-2117.2007.00344.x

Lucente, C.C., Pini, G.A., 2003. Anatomy and emplacement mechanism of a large submarine slide within a Miocene foredeep in the northern Apennines, Italy: A field perspective. American Journal of Science 303, 565.

Madof, A.S., Christie-Blick, N., Anders, M.H., 2009. Stratigraphic controls on a

salt-withdrawal intraslope minibasin, north-central Green Canyon, Gulf of Mexico: Implications for misinterpreting sea level change. Bulletin 93, 535–561. https://doi.org/10.1306/12220808082

Martinsen, O.J., 1989. Styles of soft-sediment deformation on a Namurian (Carboniferous) delta slope, Western Irish Namurian Basin, Ireland. Geological Society, London, Special Publications 41, 167–177. https://doi.org/10.1144/GSL.SP.1989.041.01.13

Martinsen, O.J., Bakken, B., 1990. Extensional and compressional zones in slumps and slides in the Namurian of County Clare, Ireland. Journal of the Geological Society 147, 153–164. https://doi.org/10.1144/gsjgs.147.1.0153

Maselli, V., Kneller, B., 2018. Bottom currents, submarine mass failures and halokinesis at the toe of the Sigsbee Escarpment (Gulf of Mexico): Contrasting regimes during lowstand and highstand conditions? Marine Geology 401, 36–65. https://doi.org/10.1016/j.margeo.2018.04.001

Masson, D.G., Harbitz, C.B., Wynn, R.B., Pedersen, G., Løvholt, F., 2006. Submarine landslides: processes, triggers and hazard prediction. Philosophical Transactions of the Royal Society A: Mathematical, Physical and Engineering Sciences 364, 2009.

Masson, D.G., Watts, A.B., Gee, M.J.R., Urgeles, R., Mitchell, N.C., Le Bas, T.P., Canals, M., 2002. Slope failures on the flanks of the western Canary Islands. Earth-Science Reviews 57, 1–35.

Masson, D.G., Wynn, R.B., Talling, P.J., 2010. Large landslides on passive continental margins: processes, hypotheses and outstanding questions. Submarine Mass Movements and Their Consequences 153–165.

McAdoo, B.G., Pratson, L.F., Orange, D.L., 2000. Submarine landslide geomorphology, US continental slope. Marine Geology 169, 103–136.

McHugh, C.M.G., Damuth, J.E., Mountain, G.S., 2002. Cenozoic mass-transport facies and their correlation with relative sea-level change, New Jersey continental margin. Marine Geology 184, 295–334. https://doi.org/10.1016/S0025-3227(01)00240-7

Meiburg, E., Kneller, B., 2010. Turbidity Currents and Their Deposits. Annu. Rev. Fluid Mech. 42, 135–156. https://doi.org/10.1146/annurev-fluid-121108-145618

Mienert, J., Berndt, C., Laberg, J.S., Vorren, T.O., 2002. Slope instability of continental margins. Ocean Margin Systems 179–193.

Mienert, J., Posewang, J., Baumann, M., 1998. Gas hydrates along the northeastern Atlantic margin: possible hydrate-bound margin instabilities and possible release of methane. Geological Society, London, Special Publications 137, 275.

Mienert, J., Vanneste, M., Bunz, S., Andreassen, K., Haflidason, H., Sejrup, H.P., 2005. Ocean warming and gas hydrate stability on the mid-Norwegian margin at the Storegga Slide. Marine and Petroleum Geology 22, 233–244.

Milkov, A.V., Sassen, R., Novikova, I., Mikhailov, E., 2000. Gas hydrates at minimum stability water depth in the Gulf of Mexico: significance to geohazard assessment. GCAGS Tranactions 50. https://doi.org/10.1306/2DC40C89-0E47-11D7-8643000102C1865D

Miramontes, E., Sultan, N., Garziglia, S., Jouet, G., Pelleter, E., Cattaneo, A., 2018. Altered volcanic deposits as basal failure surfaces of submarine landslides. Geology 46, 663–666. https://doi.org/10.1130/G40268.1

Mitchell, N.C., Masson, D.G., Watts, A.B., Gee, M.J.R., Urgeles, R., 2002. The morphology of the submarine flanks of volcanic ocean islands:: A comparative study of the Canary and Hawaiian hotspot islands. Journal of volcanology and geothermal research 115, 83–107.

Moernaut, J., De Batist, M., 2011. Frontal emplacement and mobility of sublacustrine landslides: Results from morphometric and seismostratigraphic analysis. Marine Geology 285, 29–45. https://doi.org/10.1016/j.margeo.2011.05.001

Moore, J.G., Normark, W.R., Holcomb, R.T., 1994. Giant Hawaiian underwater landslides. Science-AAAS-Weekly Paper Edition-including Guide to Scientific Information 264, 46–47.

Morley, C.K., 2009. Growth of folds in a deep-water setting. Geosphere 5, 59–89. https://doi.org/10.1130/GES00186.1

Morley, C.K., King, R., Hillis, R., Tingay, M., Backe, G., 2011. Deepwater fold and thrust belt classification, tectonics, structure and hydrocarbon prospectivity: A review. Earth-Science Reviews 104, 41–91. https://doi.org/10.1016/j.earscirev.2010.09.010

Moscardelli, L., Wood, L., 2008. New classification system for mass transport complexes in offshore Trinidad. Basin Research 20, 73–98.

Moscardelli, L., Wood, L., Mann, P., 2006. Mass-transport complexes and associated processes in the offshore area of Trinidad and Venezuela. AAPG Bulletin 90, 1059–1088. https://doi.org/10.1306/02210605052

Mulder, T., Cochonat, P., 1996. Classification of offshore mass movements. Journal of Sedimentary Research 66, 43–57.

Mulder, T., Syvitski, J.P.M., 1995. Turbidity currents generated at river mouths during exceptional discharges to the world oceans. The Journal of Geology 103, 285–299.

Nemec, W., 1990. Aspects of sediment movement on steep delta slopes.

Nittrouer, C.A., 2007. Continental margin sedimentation: from sediment transport to sequence stratigraphy. Wiley-Blackwell.

Norem, H., Locat, J., Schieldrop, B., 1990. An approach to the physics and the modelling of submarine landslides. Marine Geotechnology 9, 93–111.

Normark, W.R., Carlson, P.R., 2003. Giant submarine canyons: Is size any clue to their importance in the rock record? Extreme Depositional Environments: Mega End Members in Geologic Time 175–190.

Normark, W.R., Piper, D.J.W., 1991. Initiation processes and flow evolution of turbidity currents: implications for the depositional record. From Shoreline to Abyss: SEPM, Special Publication 46, 207–230.

O'Brien, P.E., Mitchell, C.H., Nguyen, D., Langford, R.P., 2018. Mass Transport Complexes on a Cenozoic paleo-shelf edge, Gippsland basin, southeastern Australia. Marine and Petroleum Geology 98, 783–801. https://doi.org/10.1016/j.marpetgeo.2018.08.029

Ogata, K., Mutti, E., Pini, G.A., Tinterri, R., 2012. Mass transport-related stratal disruption within sedimentary mélanges: Examples from the northern Apennines (Italy) and south-central Pyrenees (Spain). Tectonophysics 568, 185–199.

Orange, D.L., Breen, N.A., 1992. The effects of fluid escape on accretionary wedges 2. Seepage force, slope failure, headless submarine canyons, and vents. Journal of Geophysical Research 97, 9277–9295.

Orange, D.L., McAdoo, B.G., Casey Moore, J., Tobin1, H., Screaton2, E., Chezar, H., Lee, H., Reid, M., Vail, R., 1997. Headless submarine

canyons and fluid flow on the toe of the Cascadia accretionary complex. Basin Research 9, 303–312. https://doi.org/10.1046/j.1365-2117.1997.00045.x

Ortiz-Karpf, A., Hodgson, D.M., Jackson, C.A.-L., McCaffrey, W.D., 2018a. Mass-transport complexes as markers of deep-water fold-and-thrust belt evolution: insights from the southern Magdalena fan, offshore Colombia. Basin Res 30, 65–88. https://doi.org/10.1111/bre.12208

Ortiz-Karpf, A., Hodgson, D.M., Jackson, C.A.-L., McCaffrey, W.D., 2018b. Mass-transport complexes as markers of deep-water fold-and-thrust belt evolution: insights from the southern Magdalena fan, offshore Colombia. Basin Res 30, 65–88. https://doi.org/10.1111/bre.12208

Osborne, M.J., Swarbrick, R.E., 1997. Mechanisms for generating overpressure in sedimentary basins: a reevaluation. AAPG bulletin 81, 1023–1041.

Paull, C.K., Caress, D.W., Lundsten, E., Gwiazda, R., Anderson, K., McGann, M., Conrad, J., Edwards, B., Sumner, E.J., 2013. Anatomy of the La Jolla Submarine Canyon system; offshore southern California. Marine Geology 335, 16–34. https://doi.org/10.1016/j.margeo.2012.10.003

Pedley, K.L., Barnes, P.M., Pettinga, J.R., Lewis, K.B., 2010. Seafloor structural geomorphic evolution of the accretionary frontal wedge in response to seamount subduction, Poverty Indentation, New Zealand. Marine Geology 270, 119–138. https://doi.org/10.1016/j.margeo.2009.11.006

Piper, D.J.W., Shor, A.N., Farre, J.A., O'Connell, S., Jacobi, R., 1985. Sediment slides and turbidity currents on the Laurentian Fan: Sidescan sonar investigations near the epicenter of the 1929 Grand Banks earthquake. Geology 13, 538.

Posamentier, Henry W., Martinsen, O.J., 2011. The character and genesis of submarine mass-transport deposits: insights from outcrop and 3d seismic data, in: Shipp, R.C., Posamentier, H. W. (Eds.), Mass-Transport Deposits in Deepwater Settings, SEPM Special Publication, 96. pp. 7–38.

Prior, D.B., Bornhold, B.D., Coleman, J.M., Bryant, W.R., 1982. Morphology of a submarine slide, Kitimat Arm, British Columbia. Geology 10, 588–592. https://doi.org/10.1130/0091-7613(1982)10<588:MOASSK>2.0.CO;2

Prior, D. B, Bornhold, B.D., Johns, M.W., 1986. Active sand transport along a fjord-bottom channel, Bute Inlet, British Columbia. Geology 14, 581.

Prior, D.B., Bornhold, B.D., Johns, M.W., 1984. Depositional characteristics of a submarine debris flow. The Journal of Geology 92, 707–727.

Prior, D.B., Coleman, J.M., 1984. Submarine landslides, in: Proceedings of the 4th International Symposium on Landslides, Toronto. pp. 179–196.

Prior, D.B., Coleman, J.M., Programs, U.States.O. of N.Research.G., Louisiana State University (Baton Rouge, La.). C.S.I., 1979. Submarine landslides-geometry and nomenclature. Coastal Studies Institute, Center for Wetland Resources, Louisiana State Univ.

Prior, D. B., Yang, Z.S., Bornhold, B.D., Keller, G.H., Lin, Z.H., Wiseman, W.J., Wright, L.D., Lin, T.C., 1986. The subaqueous delta of the modern Huanghe (Yellow River). Geo-Marine Letters 6, 67–75.

Reagan, M.T., Moridis, G.J., 2007. Oceanic gas hydrate instability and dissociation under climate change scenarios. Geophys. Res. Lett 34, L22709.

Reeder, D.B., Ma, B.B., Yang, Y.J., 2011. Very large subaqueous sand dunes on the upper continental slope in the South China Sea generated by

episodic, shoaling deep-water internal solitary waves. Marine Geology 279, 12–18. https://doi.org/10.1016/j.margeo.2010.10.009

Riboulot, V., Imbert, P., Cattaneo, A., Voisset, M., 2019. Fluid escape features as relevant players in the enhancement of seafloor stability? Terra Nova ter.12425. https://doi.org/10.1111/ter.12425

Richardson, S.E.J., Davies, R.J., Allen, M.B., Grant, S.F., 2011. Structure and evolution of mass transport deposits in the South Caspian Basin, Azerbaijan. Basin Research. https://doi.org/10.1111/j.1365-2117.2011.00508.x

Rodríguez-Ochoa, R., Nadim, F., Hicks, M.A., 2015. Influence of weak layers on seismic stability of submarine slopes. Marine and Petroleum Geology 65, 247–268. https://doi.org/10.1016/j.marpetgeo.2015.04.007

Rowan, M.G., Peel, F.J., Vendeville, B.C., 2004. Gravity-driven fold belts on passive margins, in: McClay, K.R. (Ed.), Thrust Tectonics and Hydrocarbon Systems, AAPG Memoirs, 82. pp. 157–182.

Ruh, J.B., 2016. Submarine landslides caused by seamounts entering accretionary wedge systems. Terra Nova 28, 163–170. https://doi.org/10.1111/ter.12204

Sawyer, D.E., DeVore, J.R., 2015. Elevated shear strength of sediments on active margins: Evidence for seismic strengthening: ACTIVE MARGIN ELEVATED SHEAR STRENGTH. Geophys. Res. Lett. 42, 10,216-10,221. https://doi.org/10.1002/2015GL066603

Sawyer, D.E., Flemings, P.B., Dugan, B., Germaine, J.T., 2009. Retrogressive failures recorded in mass transport deposits in the Ursa Basin, Northern Gulf of Mexico. Journal of Geophysical Research 114, B10102. https://doi.org/10.1029/2008JB006159.

Sawyer, D.E., Mason, R.A., Cook, A.E., Portnov, A., 2019. Submarine Landslides Induce Massive Waves in Subsea Brine Pools. Sci Rep 9, 128. https://doi.org/10.1038/s41598-018-36781-7

Sayago-Gil, M., Long, D., Fernández-Salas, L.M., Hitchen, K., López-González, N., Díaz-del-Río, V., Durán-Mu\ noz, P., 2010. Geomorphology of the Talismán Slide (Western slope of Hatton Bank, NE Atlantic Ocean). Submarine Mass Movements and Their Consequences 289–300.

Scarselli, N., McClay, K., Elders, C., 2020. Composite Slope Failures: Seismic Examples From the NW Shelf of Australia, in: Ogata, K., Festa, A., Pini, G.A. (Eds.), Submarine Landslides: Subaqueous Mass-Transport Deposits from Outcrops to Seismic Profiles, American Geophysical Union, Geophysical Monograph. John Wiley & Sons, Inc., pp. 261–276.

Scarselli, N., McClay, K., Elders, C., 2016. Seismic geomorphology of cretaceous megaslides offshore Namibia (Orange Basin): Insights into segmentation and degradation of gravity-driven linked systems. Marine and Petroleum Geology 75, 151–180. https://doi.org/10.1016/j.marpetgeo.2016.03.012

Scarselli, Nicola, McClay, K., Elders, C., 2013. Submarine slide and slump complexes, Exmouth Plateau, NW Shelf of Australia, in: Keep, M., Moss, S.J. (Eds.), The Sedimentary Basins of Western Australia IV: Proceedings of the Petroleum Exploration Society of Australia Symposium. Perth, WA.

Scarselli, N., McClay, K., Elders, C., 2013. Submarine slide and slump complexes, Exmouth Plateau, NW shelf of Australia, in: The Sedimentary Basins of Western Australia IV: Proceedings of the Petroleum Exploration

Society of Australia Symposium. Perth, WA. pp. 1–20.

Seed, H.B., Rahman, M.S., 1978. Wave-induced pore pressure in relation to ocean floor stability of cohesionless soils. Marine Georesources & Geotechnology 3, 123–150.

Shepard, F.P., 1981. Submarine canyons: multiple causes and long-time persistence.

Shepard, F.P., 1972. Submarine canyons. Earth-Science Reviews 8, 1–12. https://doi.org/10.1016/0012-8252(72)90032-3

Stoker, M.S., Wilson, C.R., Howe, J.A., Bradwell, T., Long, D., 2010. Paraglacial slope instability in Scottish fjords: examples from Little Loch Broom, NW Scotland. Geological Society, London, Special Publications 344, 225.

Stow, D.A.V., 1986. Deep clastic seas. Sedimentary Environments and Facies 2, 399–444.

Stow, D.A.V., 1985. Deep-sea clastics: where are we and where are we going? Geological Society London Special Publications 18, 67.

Stow, D.A.V., Mayall, M., 2000. Deep-water sedimentary systems: New models for the 21st century. Marine and Petroleum Geology 17, 125–135.

Strachan, L.J., 2002. Slump-initiated and controlled syndepositional sandstone remobilization: an example from the Namurian of County Clare, Ireland. Sedimentology 49, 25–41.

Strachan, L.J., Alsop, G.I., 2006. Slump folds as estimators of palaeoslope: a case study from the Fisherstreet Slump of County Clare, Ireland. Basin Research 18, 451–470. https://doi.org/10.1111/j.1365-2117.2006.00302.x

Syvitski, J.P.M., Burrell, D.C., Skei, J.M., 1987. Fjords: processes and products.

Syvitski, J.P.M., Farrow, G.E., 1989. Fjord sedimentation as an analogue for small hydrocarbon-bearing fan deltas. Geological Society, London, Special Publications 41, 21–43. https://doi.org/10.1144/GSL.SP.1989.041.01.03

Talling, P.J., Wynn, R.B., Masson, D.G., Frenz, M., Cronin, B.T., Schiebel, R., Akhmetzhanov, A.M., Dallmeier-Tiessen, S., Benetti, S., Weaver, P.P.E., Georgiopoulou, A., Zuhlsdorff, C., Amy, L.A., 2007. Onset of submarine debris flow deposition far from original giant landslide. Nature 450, 541–544. https://doi.org/10.1038/nature06313

Terzaghi, K., 1962. Stability of Steep Slopes on Hard Unweathered Rock. Géotechnique 12, 251–270. http://dx.doi.org/10.1680/geot.1962.12.4.251

Tilling, R.I., Dvorak, J.J., 1993. Anatomy of a basaltic volcano. Nature 363, 125–133.

Tilling, R.I., Heliker, C., Wright, T.L., 1987. Eruptions of Hawaiian volcanoes. US Geolog. Survey, Federal Center.

Tournadour, E., Mulder, T., Borgomano, J., Hanquiez, V., Ducassou, E., Gillet, H., 2015. Origin and architecture of a Mass Transport Complex on the northwest slope of Little Bahama Bank (Bahamas): Relations between off-bank transport, bottom current sedimentation and submarine landslides. Sedimentary Geology 317, 9–26. https://doi.org/10.1016/j.sedgeo.2014.10.003

Twichell, D.C., Chaytor, J.D., Ten Brink, U.S., Buczkowski, B., 2009. Morphology of late Quaternary submarine landslides along the US Atlantic continental margin. Marine Geology 264, 4–15.

Twichell, D.C., Roberts, D.G., 1982. Morphology, distribution, and development of submarine canyons on the United States Atlantic continental slope between Hudson arid Baltimore Canyons. Geology 10, 408.

van Weering, T.C.E., Nielsen, T., Kenyon, N.H., Akentieva, K., Kuijpers, A.H., 1998. Sediments and sedimentation at the NE Faeroe continental margin; contourites and large-scale sliding. Marine Geology 152, 159–176. https://doi.org/16/S0025-3227(98)00069-3

Varnes, D.J., 1958. Landslide types and processes. Highway Research Board Special Report.

Webb, B.C., Cooper, A.H., 1988. Slump folds and gravity slide structures in a Lower Palaeozoic marginal basin sequence (the Skiddaw Group), NW England. Journal of structural geology 10, 463–472.

Welbon, A.I.F., Brockbank, P.J., Brunsden, D., Olsen, T.S., 2007. Characterizing and producing from reservoirs in landslides: challenges and opportunities, in: Barr, D., Walsh, J.J., Knipe R.J. (Eds.), Structurally Complex Reservoirs, Geological Society London, Special Publications, 292. pp. 49–74.

Woodcock, N.H., 1979. The use of slump structures as palaeoslope orientation estimators. Sedimentology 26, 83–99.

Wright, L.D., Coleman, J.M., Programs, U.States.O. of N.Research.G., Louisiana State University (Baton Rouge, La.). C.S.I., 1973. Variations in morphology of major river deltas as functions of ocean wave and river discharge regimes.

Xu, W., Germanovich, L.N., 2006. Excess pore pressure resulting from methane hydrate dissociation in marine sediments: A theoretical approach. Journal of geophysical research 111, B01104.